SO_2-Resistant Immobilized Amine Sorbents for CO_2 Capture

Final Technical Report to the

Department of Energy,

DE-FE0001780

Jan. 1, 2010 - Aug. 31, 2013

Principal investigator: Steven S. C. Chuang

Organized by: Uma Tumuluri

Department of Polymer Science

The University of Akron

170 University Ave., Akron, OH, 44325

January, 2014

ABSTRACT

The solid amine sorbent for CO_2 capture process has advantages of simplicity and low operating cost compared to the MEA (monoethanolamine) process. Solid amine sorbents reported so far suffered from either low CO_2 capture capacity or low stability in the flue gas environment. This project is aimed at developing a SO_2-resistant solid amine sorbent for capturing CO_2 from coal–fired power plants with SCR/FGD which emits SO_2 ranging from 15 to 30 ppm and NO ranging from 5 to 10 ppm.

The amine sorbent we developed in a previous project degraded rapidly with 65% decrease in the initial capture capacity in presence of 1% SO_2. This amine sorbent was further modified by coating with polyethyleneglycol (PEG) to increase the SO_2-resistance. Polyethylene glycol (PEG) was found to decrease the SO_2-amine interaction, resulting in the decrease in the maximum SO desorption temperature (T_{max}) of amine sorbent. The PEG-coated amine sorbent exhibited higher stability with only 40% decrease in the initial capture capacity compared to un-coated amine sorbents. The cost of the solid amine sorbent developed in this project is estimated to be less than $7.00/lb; the sorbent exhibited CO_2 capture capacity more than 2.3 mmol/g. The results of this study provided the scientific basis for further development of SO_2-resistant sorbents.

Table of contents

1. Executive summary

The objective of this project is to develop an efficient and low-cost CO_2 capture solid sorbent which is highly resistant to SO_2 poisoning and thermal degradation. The solid amines developed in this project consist of the low cost organic amine, degradation inhibitor, and linker to bind organic amine on the surface of the porous oxides. The cost of the sorbent is estimated to be less than $7.00/lb; the sorbent exhibited CO_2 capture capacity more than 2.3 mmol/g. Extensive reproducibility studies have shown that the amine-immobilized solid sorbents we developed exhibited good CO_2 capture capacity and moderate stability.

The process of CO_2 and SO_2 capture on this sorbent follows the acid-base interaction chemistry. We have further studied the interaction of SO_2 with the amine solid sorbent by both infrared spectroscopy and mass spectrometry. This study provided an insight into the process of SO_2 capture and determined the binding strength between SO_2 and amine species on the sorbent.

Fundamental SO_2 capture study on liquid films showed that the presence of PEG improved the SO_2 capture capacities and stability of tetraethylenepentamine (TEPA) liquid film. Polyethylene glycol (PEG) decreases the SO_2-amine interaction, resulting in the decrease in the maximum SO desorption temperature (T_{max}) of TEPA films. The high stability of the TEPA/PEG (1:2) film is attributed to the decrease in the strength of SO_2-amine interaction with increasing amounts of PEG in the film. These results are used in designing SO_2 resistant amine solid sorbent. The amine sorbent degraded rapidly with 65% decrease in the initial capture capacity where as the PEG-coated amine sorbent exhibited higher stability with only 40% decrease in the initial capture capacity. The results of this study provided the scientific basis for further development of SO_2-resistant sorbents.

This project has resulted in the following publications

Publications:

1. Srikanth, C. S.; Chuang, S. S. C. *The Journal of Physical Chemistry C* **2013**, 117, 9196
2. Isenberg, M., Chuang, S. S. C. Ind. Eng. Chem. Res., **2013**, 52, 12530
3. Tumuluri, U., Chuang, S. S. C. *to be submitted in Langmuir*

Patent Applications:

Low Cost ImmobilizedAmine Regenerable Solid Sorbent
7/1/2011 N/A Chuang, Steven S. (PI) 13/978,657 US UA 812 PCT US Filed Nationalized PCT

Low Cost ImmobilizedAmine Regenerable Solid Sorbents
1/7/2011 N/A Chuang, Steven S. (PI) 201180068193.9 CN UA 812 PCT CN Filed Nationalized PCT

Low Cost ImmobilizedAmine Regenerable Solid Sorbents
1/7/2011 N/A Chuang, Steven S. (PI) PCT/US2010/05427

2. Introduction

The continuous rise in CO_2 concentration and its strong effect on global warming demands cost-effective approaches to stabilize the CO_2 concentration in the atmosphere. Examination of various sources of CO_2 emissions revealed that more than 33% of global CO_2 emissions originate from coal-fired power plants which represent the largest stationary source of CO_2 [1]. Depending on operating conditions and the type of coal burned, CO_2 concentration in the power plant flue gas varies from 10-15 %, NO from 1500-2500 ppm, and SO_2 from 500-2000 ppm.[2] NO is removed by the selective catalytic reduction (i.e. SCR) while SO_2 is captured by the flue gas desulfurization (i.e., FGD) unit.[3] SO_2 in the SCR/FGD-treated flue gas ranges from 15 to 30 ppm; NO ranges from 5 to 10 ppm.[4]

CO_2 capture using amine solid sorbents is a promising technology for CO_2 capture from point sources because of its (i) low energy requirements, (ii) low toxicity of the materials, and (iii) high capture capacity, and (iv) possibility for further modification for high stability.[5] The objective of this project is to develop an efficient and low-cost CO_2 capture solid sorbent which is highly resistant to SO_2 poisoning and thermal degradation.

Success Criteria:

Develop amine solid capable of capturing 1.5 mmol/g of CO_2 with less than 10% degradation in 100 adsorption/desorption cycles under 3,000 h^{-1} space velocity with a simulated flue gas containing 15-30 ppm SO_2.

The success criteria were not thoroughly tested. We found that amine sorbents, we developed, exhibited low stability with only 40% decrease in the initial capture capacity with 1% SO_2. Further study on the sorbent stability in the 15-30 ppm range is needed. This study was not completed due to the equipment limitation.

3. Experimental methods

3.1. In-situ DRIFTS study on the SO_2 capture on PEG-400 liquid films

Figure 1 shows the experimental apparatus consisting of (i) a gas flow manifold which includes mass flow meters and a controller, a four port-valve, and a six-port valve, (ii) DRIFT (Diffuse Reflectance Infrared Fourier Transform, Spectra-Tech) cell with a reflection plate accessory, containing PEG400 in a form of a thin film, and placed in a Nicolet 6700 FT-IR bench (IR), (iii) Pfeiffer QMS 200 quadruple mass spectrometer (MS), and (iv) signal input-output module that controls the 4-port and 6-port valves position, DRIFT cell temperature, and heating rate.

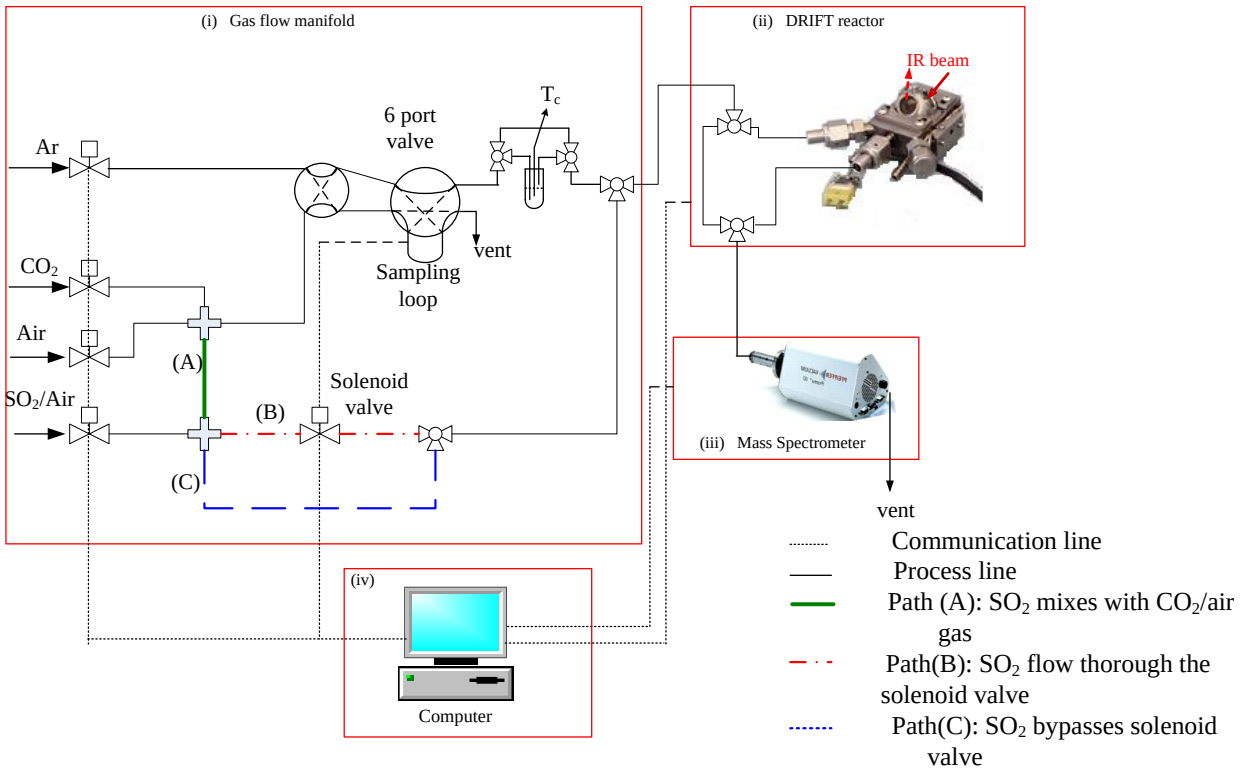

Figure 1: Experimental apparatus for SO_2 capture PEG liquid films

SO_2 capture study:

SO_2 capture was performed on a liquid thin film of polyethylene glycol with an average molecular weight of 400, herein referred to as PEG-400. 7.7 mg of PEG400 was casted on a 9.5mm diameter aluminum disk. SO_2 adsorption was carried out for 10 minutes by flowing 50 cm^3/min of an air stream containing 260 ppm of SO_2. The adsorption was followed by reactor

evacuation with Ar for 3 minutes. Temperature programmed desorption (TPD) at 120 ^{o}C was performed after the reactor evacuation in the presence of flowing Ar. The formation and desorption of SO_2 adsorbed species on the thin film was continuously monitored by Fourier-transform infrared spectroscopy (FTIR), coupled with mass spectroscopy (MS) of the reactor effluent gases.

3.2. In-situ ATR studies on the effect of PEG on SO_2 adsorption of TEPA liquid films

The experimental apparatus shown in Figure 2 consists of (i) a reactant gas metering system (Brooks Instruments 5850 flow controllers) (ii) a gas sampling system including 4-port and 6-port valves (iii) Attenuated Total Reflectance accessory (ATR-IR, Harrick Scientific) equipped with ZnSe window (4.35 cm x 0.63 cm) placed inside a Fourier Transform Infrared spectroscopy (FTS6700 FTIR, Thermo-Nicolet) and (iv) a mass spectrometer (MS, Pfeiffer Omnistar^{TM}). The 4-port valve is used to switch the gases between SO_2 and N_2 and 6-port value is used to inject 3 cm^3 of SO_2/N_2 gases in to pure N_2 flow for the calibration purpose.

Preparation and characterization of thin films:

Thin films of tetraethylenepentamine (TEPA) and polyethylene glycol (PEG) with molecular weight 200, herein referred to as PEG-400 with weight ratios of 2:1, 1:1 and 1:2 were used for the SO_2adsorption and desorption studies. 0.057 M solution of TEPA/ethanol and PEG/ethanol was casted on ATR window. The procedures for the preparation of thin film involves (i) casting TEPA/ethanol solution ATR window and allow 15 min to evaporate ethanol (ii) injecting PEG/ethanol over the TEPA layer and allow 15 min to evaporate ethanol. For example, 2:1 ratio TEPA/PEG film was prepared by injecting 0.4 cm^3 of TEPA/ethanol followed by 0.2 cm^3 of PEG/ethanol. The thin film was heated to 100 ^{o}C at 10 ^{o}C/min and hold for 15 min under N_2 flow of 100 cm^3/min to completely evaporate ethanol and cooled down to 50 ^{o}C for the adsorption study.

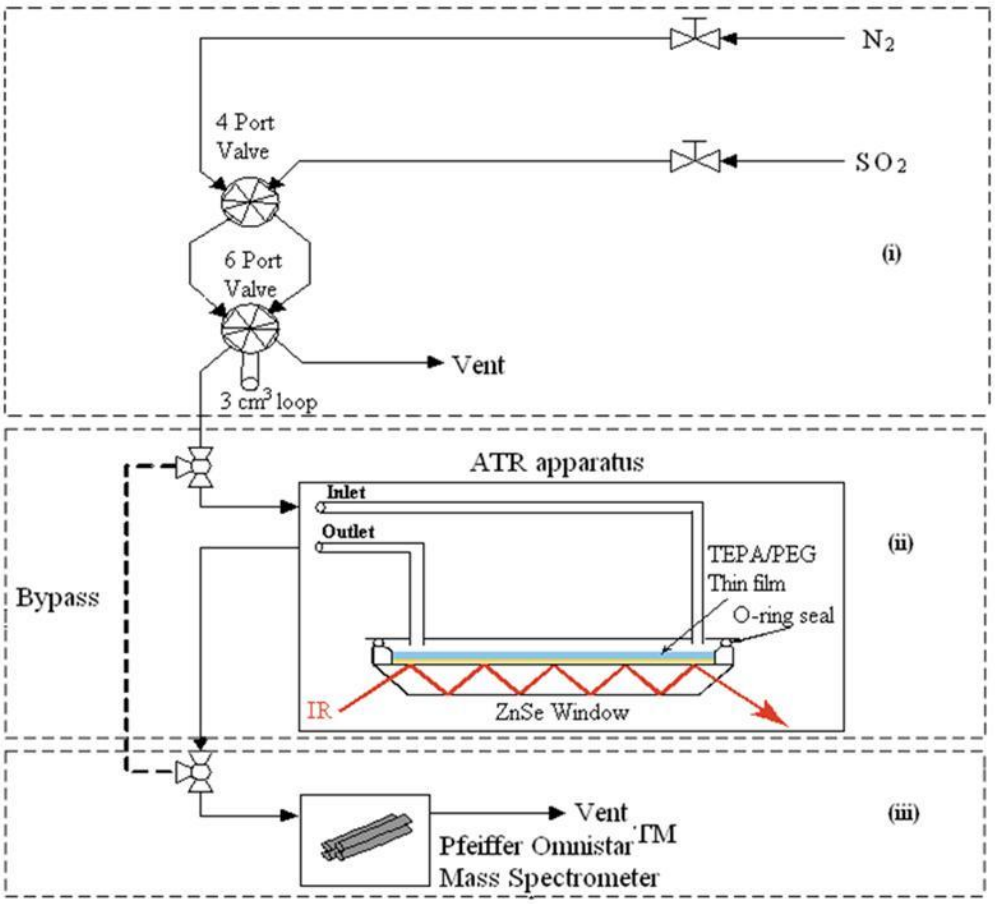

Figure 2: Experimental Apparatus

SO_2 adsorption and desorption study on thin films:

The SO_2 capture studies on TEPA/PEG films were performed for 3 adsorption/desorption cycles to determine the capture capacity and stability of the thin films. The SO_2 adsorption and desorption on thin films are carried out by the following steps (i) exposing to 100 cm^3/min N_2 flow for 30 min at 50 ^oC to attain a stable MS baseline and IR background spectra (ii) step switching the gas flow from N_2 to 30 cm^3/min flow of SO_2 (Anhydrous 99.99%) at 50 ^oC for 30 min by the 4-port value (iii) switching back to N_2 flow at 100 cm^3/min to remove weakly adsorbed SO_2 for 20 min, (iv) pulsing four 3 cm^3 of SO_2 in the same N_2 flow by 6 port valve for calibration (v) performing temperature programmed desorption (TPD) from 50-100 ^oC at 5 ^oC/min in flowing N_2, holding at 100 ^oC for 20 min and cooling back to 50 ^oC. The structure of adsorbed species and their intensities are monitored by ATR-IR. The single beam spectra of thin films were collected by 32 co-adding scans and a resolution of 4 cm^{-1} at a rate of 6 scans/min. The absorbance spectrum was obtained by the equation Abs = -log (I/I_0) where I is single beam spectrum of interest and I_0 is single beam spectrum of the fresh film after pretreatment with N_2. The effluent gases from the ATR were monitored by MS. The capture capacity of the films was calculated by dividing the area under the SO_2 profile by the amount of SO_2 injected.

3.3. In-situ DRIFTS study on the effect of water on SO_2 capture of TEPA liquid film.

TEPA thin films were prepared by casting 5 µl of TEPA or TEPA/H_2O solution on a metal cup with diameter of 18 mm and depth of 3 mm. The metal cup was placed in a DRIFT cell for SO_2 adsorption and desorption study. The DRIFT cell was set to batch mode by closing the inlet and outlet valves. SO_2 adsorption on the thin film was carried out by injecting 2 cm^3 of pure SO_2 in to the DRIFT cell by a gas syringe. The gas phase SO_2 was allowed to equilibrate for 2 min. The DRIFT cell was switched back to continuous flow mode by opening the inlet and outlet valves, and the gas phase SO_2 was purged for 3 min under flowing Ar. Temperature programmed desorption (TPD) was carried out by heating the sample under flowing Ar from 30-100 ^oC, holding at 100 ^oC for 3 min, and cooling down to 30 ^oC.

3.4. In-situ DRIFTS study on the effect of PEG on TPSENa sorbent

Sorbent preparation: TPSENa sorbent was prepared by impregnating SiO_2 (S) (Rodia chemicals) with TPSENa solution. TPSENa solution contains 22.5 g Tetraethylpentamine (T) (TEPA, Acros organics, 98%), 15 g Polyethylene Glycol (P) with average Mw of 200 (PEG-200, Sigma Aldrich, 99%), 4.2 g of polymer linker, 0.625 g of antioxidant, 80 g of H_2O, and 80 g of ethanol. The solution was allowed to diffuse for 30 min and the excess solution was drained off. The slurry was dried at 100^oC for 3 hours. TPSENa was coated with different concentrations of PEG by impregnating the sorbent with 1, 5 and 10 % of the weight of sorbent with PEG. The wet slurry was dried at 100^oC for 20 min to obtain TPSENa-1P, TPSENa-5P and TPSENa-10P sorbent.

Experimental apparatus: Figure 1 shows the experimental apparatus. It consists of (i) a gas flow manifold which includes mass flow meters and controller that monitor and control the flow of gases , a four port-valve for switching the inlet gas from Ar to SO_2 and a six-port valve for calibration, (ii) DRIFT cell filled with 50 mg of the sorbent placed in a Nicolet 6700 FT-IR bench (IR) and (iii) Pfeiffer QMS 200 quadruple mass spectrometer (MS) and (iv) signal input-output module that controls 4-port and 6-port valve position, DRIFT cell temperature, and heating rate.

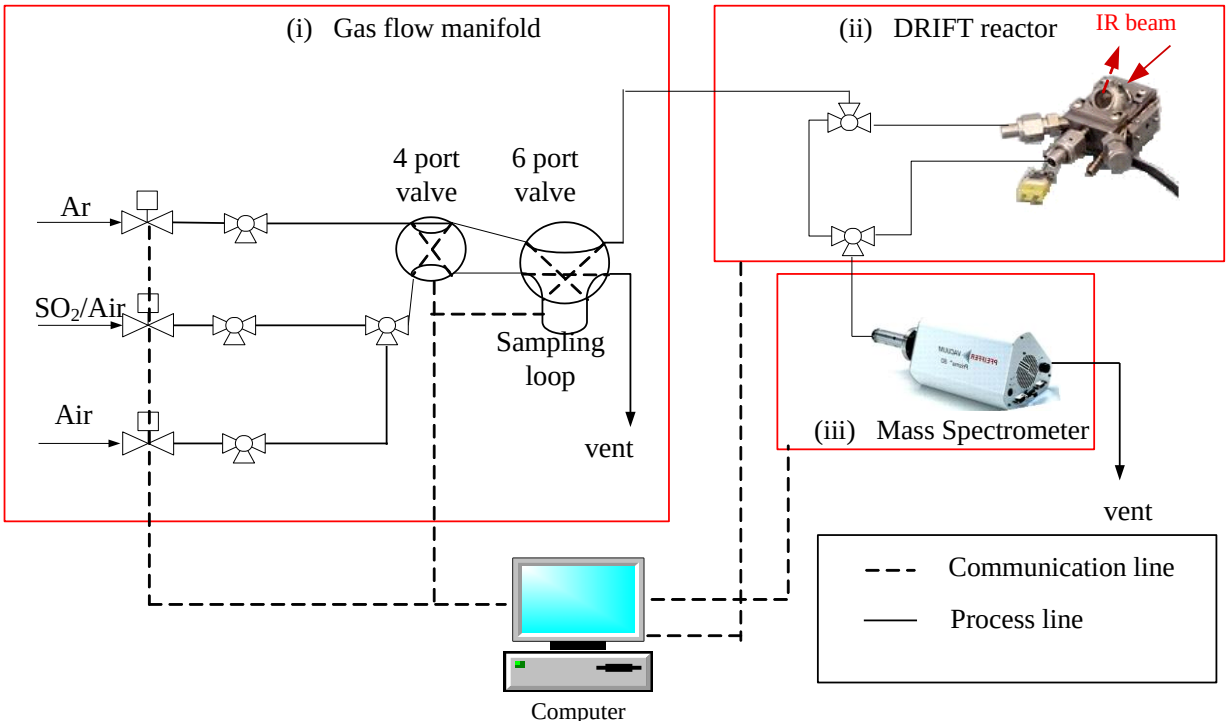

Figure 3: Experimental apparatus for SO_2 capture over TPSENa-P

SO_2 capture study: 17 cycles of SO_2 adsorption and desorption was performed on TPSENa, TPSENa-1P, TPSENa-5P, TPSENa-10P to evaluate the effect of presence of PEG at different concentrations on SO_2 capture capacity and stability of the sorbent. The sorbent was initially heated to 100^{o}C for 10 min under 150 cm^3/min Ar to remove pre-adsorbed CO_2 and H_2O. SO_2 calibration was performed at 100^{o}C by pulsing 1 and 3 cm^3 of 1vol% SO_2 via 6-port valve prior cooling down to 40^{o}C. Each cycle of SO_2 capture consisted of the following steps 1) exposing the sorbent to Ar flowing at 150 cm^3/min for 1 min, 2) Switching the inlet gas from Ar to 1 vol% SO_2 flowing at 150 cm^3/min for 5 min, 3) purging the weakly adsorbed SO_2 species with Ar flowing at 150 cm^3/min for 10 min and 4) performing temperature programmed desorption (TPD), where the sorbent was heated to 170^{o}C at 10^{o}C/min in presence of Ar. The sorbent was held at 170^{o}C for 5 min and cooled down to 40^{o}C. Changes in the surface characteristics of the sorbent were monitored continuously by DRIFT. Composition of the effluents from DRIFT was monitored by MS. The amount of SO_2 desorbed during TPD was obtained by multiplying area under SO_2 MS profile (m/e = 64) with the calibration factor. Calibration factor was obtained by dividing the volume of 1% SO_2 pulsed by the area under corresponding pulse.

3.5. In-situ DRIFTS study on the effect of SO_2 on CO_2 capture of TPSENa sorbent

Figure 4 shows the experimental apparatus. It consists of (i) a gas flow manifold which includes mass flow meters and controller, a four port-valve and a six-port valve, (ii) DRIFT cell filled with 50 mg of the sorbent placed in a Nicolet 6700 FT-IR bench (IR) and (iii) Pfeiffer QMS 200 quadruple mass spectrometer (MS) and (iv) signal input-output module that controls 4-port and 6-port valve position, DRIFT cell temperature, and heating rate.

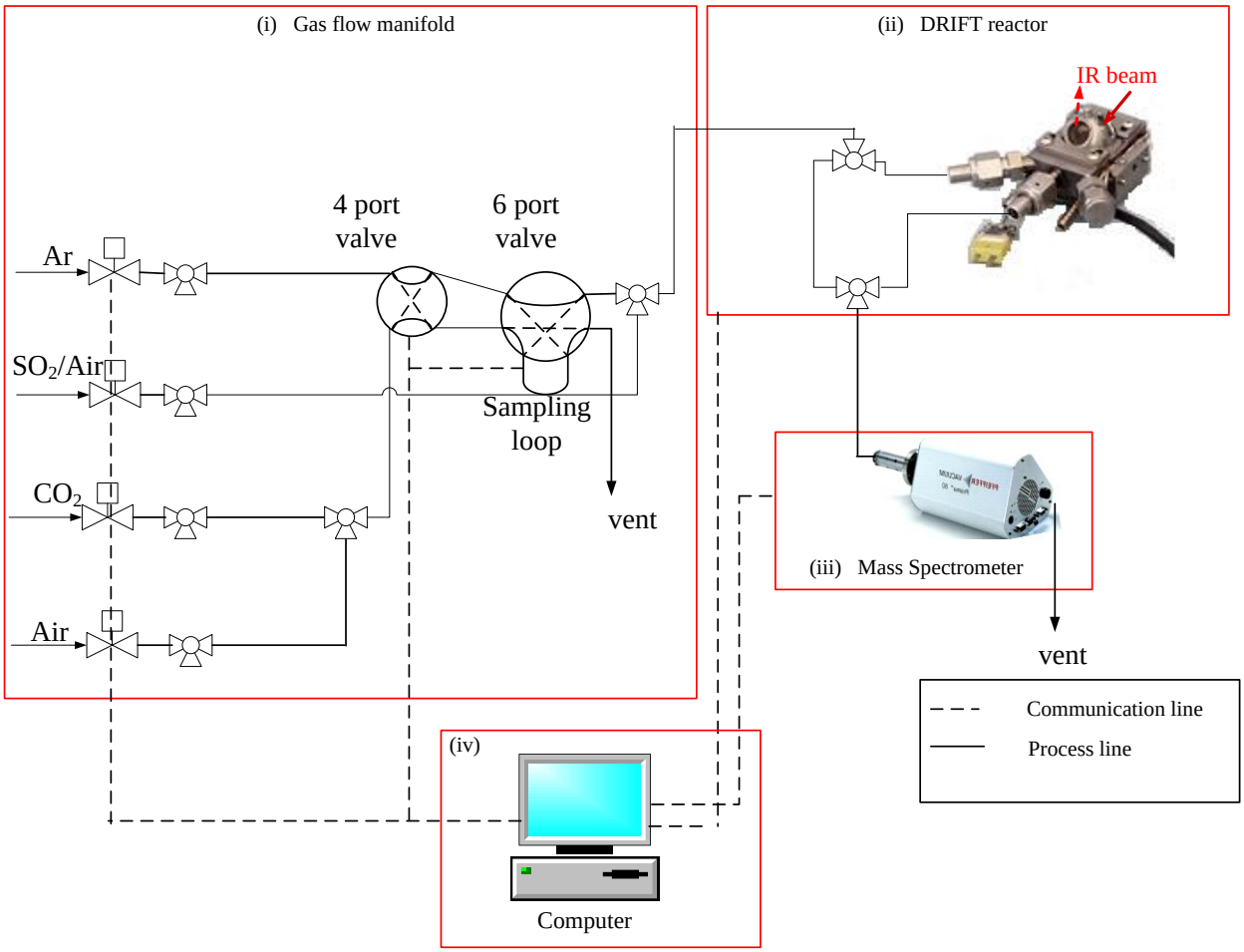

Figure 4: Experimental apparatus for CO_2 capture in presence of SO_2 over TPSENa-P

CO_2 capture study: CO_2 capture study on TPSENa-P sorbent was performed under the presence of 40 and 100 ppm SO_2 to evaluate the effect of SO_2 on the CO_2 capture capacity of the sorbent. The sorbent was initially heated to 100^oC for 10 min under 150 cm^3/min Ar to remove pre-adsorbed CO_2 and H_2O. CO_2 calibration was subsequently performed at 100^oC by pulsing 1

and 3 cm^3 of pure CO_2 via 6-port valve prior cooling down to 40 ^oC. Each cycle of CO_2 capture consisted of the following steps 1) exposing the sorbent to Ar flowing at 150 cm^3/min, 2) Switching the inlet gas from Ar to CO_2/SO_2/air for 5 min for CO_2 adsorption, 3) switching the inlet gas back to Ar to purge out weakly adsorbed CO_2 for 10 min and 4) performing temperature programmed desorption (TPD), where the sorbent was heated from 40 ^oC to 135^oC at 10^oC/min in presence of Ar. The sorbent was held at 135^oC for 5 min and cooled down to 40^oC. Changes in the surface characteristics of the sorbent were monitored continuously by DRIFT. Composition of the effluents from DRIFT was monitored by mass spectrometer. The amount of CO_2 desorbed during TPD was obtained by multiplying area under CO_2 MS profile (m/e = 44) with the calibration factor. Calibration factor was obtained by dividing the volume of pure CO_2 pulsed by the area under corresponding pulse.

3.6. In-situ DRIFTS study on the effect of presence of SO_2 and H_2O on the CO_2 capture of TPSENa sorbent

Figure **5** shows the experimental apparatus consisting of (i) a gas flow manifold which includes mass flow meters and controller, a four port-valve and a six-port valve, (ii) DRIFT cell filled with 50 mg of the sorbent placed in a Nicolet 6700 FT-IR bench (IR), (iii) Pfeiffer QMS 200 quadruple mass spectrometer (MS) ,and (iv) signal input-output module that controls 4-port and 6-port valve position, DRIFT cell temperature, and heating rate.

CO_2 capture study: CO_2 capture study on amine sorbent was performed with a simulated flue gas, a 15% CO_2/air stream, in the presence of 40 and 250 ppm SO_2 with and without the presence of water vapor. Pre-adsorbed CO_2 and H_2O were removed from the sorbent by heating to 100^oC for 10 min under the presence of Ar flowing at 150 cm^3/min. CO_2 calibration for determining CO_2 capture capacity was performed at 100^oC by pulsing 1 and 3 cm^3 of CO_2 via 6-port valve prior to cooling to 40^oC. A typical CO_2 capture cycle consists of the following steps:

- Pretreatment: The sorbent was exposed to Ar flowing at 150 cm^3/min for 1 min.

CO_2 adsorption: The DRIFT cell inlet gas is switched from Ar to the simulated flue gas flowing at 150 cm^3/min for 5 min.

- DRIFT cell purge: The DRIFT cell was purged with Ar flowing at 150 cm^3/min for 10 min to remove residual gases.
- Desorption: The sorbent was regenerated by performing temperature programmed desorption (TPD), where the sorbent was heated to 100^oC at 10^oC/min in presence of Ar. The sorbent was held at 100^oC for 5 min followed by cooling to 40^oC.

Changes in the surface characteristics of the sorbent were monitored continuously by IR spectrometer with 32 co-added scans at a resolution of 4cm^{-1}. The composition of the DRIFT

cell effluent was continuously monitored by mass spectrometer. The volume of CO_2 desorbed during TPD was obtained by multiplying the area under the CO_2 MS profile (m/e = 44) with the calibration factor. The calibration factor was calculated from a calibration curve obtained by plotting volume of CO_2 pulsed versus area under the corresponding pulse.

For the experiments involving water vapor, the inlet gas stream is bubbled through a water saturator prior to entering the DRIFT cell. Figure 1 also shows that SO_2 was introduced into the inlet gas stream along different paths, labeled A, B, and C. Allowing the SO_2 to flow through the three different paths provided insight in the role of mass flow controllers and solenoid valves have on maintaining a balanced mix of inlet gases. Table 1 provides the experimental conditions of the CO_2 capture cycles performed on the amine sorbent in presence of SO_2 and SO_2/H_2O.

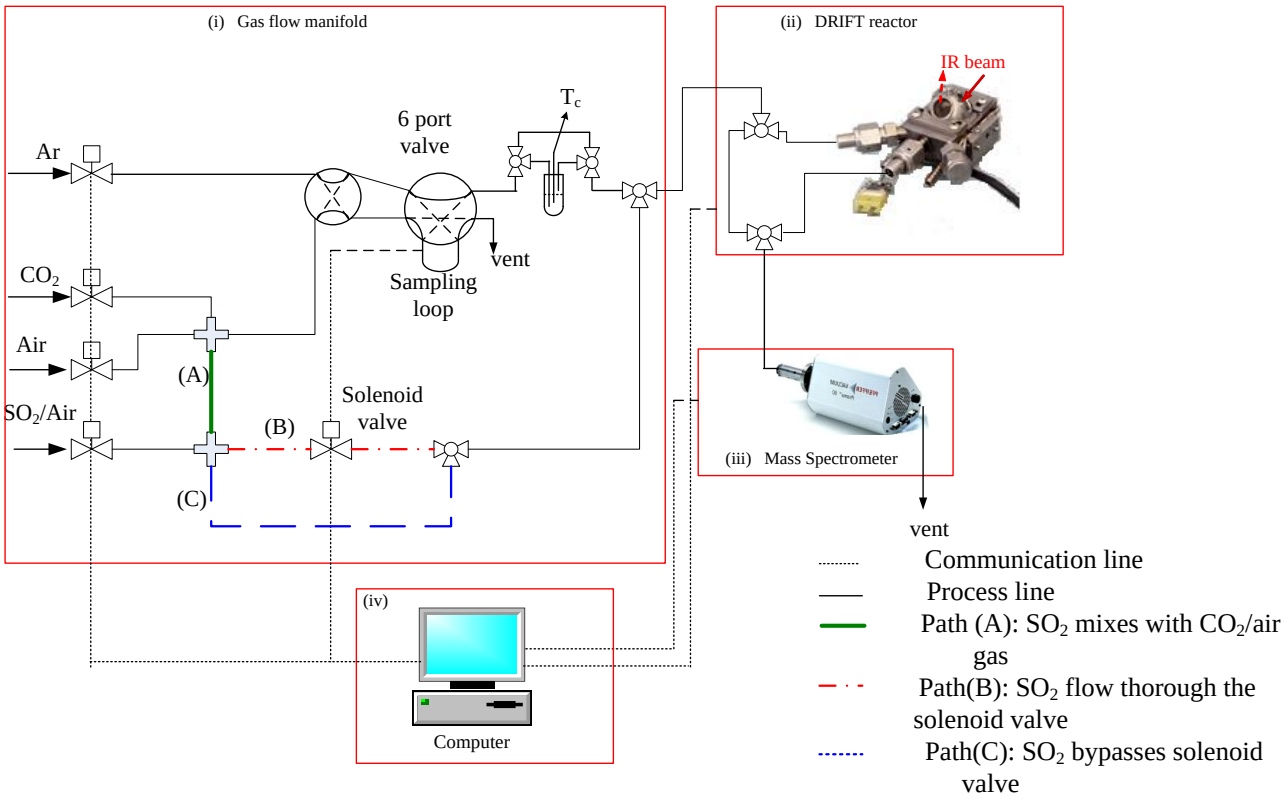

Figure 5: Experimental apparatus for CO_2 capture in presence of SO_2 over amine sorbent

Table 1: Experimental conditions for different CO_2 capture studies.

Experiment	Inlet gas stream			SO_2 flow conditions		
	Gas	Flow rate (cm^3/min)	Conc. (vol %)	Path (Fig. 1)	SO_2 mixing pt.*	SO_2 flow mode
$SO_2$40A^{dry}	CO_2 Air SO_2(260 ppm)	22.5 103.5 24	15 69 40ppm	Path A	Upstream	During adsorption (Air/CO_2/SO_2-Air)
$SO_2$40B^{dry}	CO_2 Air SO_2(260 ppm)	22.5 103.5 24	15 69 40ppm	Path B	Downstream	During adsorption (Air/CO_2 + SO_2-Air)
$SO_2$40B^{wet}	CO_2 Air SO_2(260 ppm) H_2O	22.5 103.5 24 -	15 69 40ppm 4	Path B	Downstream	During adsorption (Air/CO_2 + SO_2-Air)
$SO_2$250B^{wet}	CO_2 Air SO_2 (1%) H_2O	22.5 124.5 3.75 -	15 83 250ppm 4	Path B	Downstream	During adsorption (Air/CO_2 + SO_2-Air)
$SO_2$250C^{wet}	CO_2 Air SO_2(1%) H_2O	22.5 124.5 3.75 -	15 83 250ppm 4	Path C	Downstream	Continuous (Ar + SO_2-Air) [153] (Air/CO_2 + SO_2-Air) [150]

* Relative to 6-port valves.

3.7. In-situ FTIR study on the nature of CO_2 adsorbed species on the solid amine sorbents

Sorbent preparation: The amines used in this study are TEPA and Polyethyleneimine (PEI, Aldrich chem). PEG-200 was used as an additive. TEPA/SiO_2, PEI/SiO_2, and PEI/PEG/SiO_2 powder sorbents were prepared by mixing 2 g of silica (Tixosil 68-B, Rhodia chemicals) with 10 cm^3 of 20 vol% amine/ethanol solution. The mixture was dried for 30 min in an oven at 100 ^oC. Liquid samples were prepared by casting 5 µl of an amine/ethanol solution 0.23 M on a metal cup with 18mm diameter and 3mm depth.

Batch Calibration: The dome of a DRIFT reactor was modified by replacing the front side with Polytetrafluoroethylene (PTFE) septum to inject CO_2 gases for calibration. The powder sorbent

was pretreated at 130 ^{o}C by flowing 150 cm^{3}/min of Ar for 5 min. A 0.5 cm^{3} injection of natural gas was introduced in the reactor for internal reference. For CO_2 calibration, various volumes of CO_2 (0.5, 0.5, 1,1,1 cm^{3}) were injected, and allowed to equilibrate for 4min. The IR intensity of gas phase CO_2 at 2360 cm^{-1} after each injection was used to obtain a calibration curve. For liquid samples the calibration was carried out at 100 ^{o}C to avoid evaporation of liquids.

CO_2 adsorption/desorption: CO_2 adsorption/desorption on the powder sorbents and liquid amines consisted of (i) flowing 150 cm^{3}/min of 15% CO_2/Air for 10 min at 50 ^{o}C; (ii) switching to 150 cm^{3}/min of Ar for 5 min, and (iii) using batch temperature programmed desorption (TPD) to release the CO_2. The structure of the adsorbed CO_2 species and their intensities were determined by DRIFT. The intensity of gas phase CO_2 at the highest temperature during batch TPD was introduced into the calibration curve to obtain the CO_2 capture capacity.

HCl vapor treatment: Polytetrafluoroethylene (PTFE) septum on the DRIFT reactor was removed for the introduction of HCl vapors over the sample. The samples were saturated with 15% CO_2/Air for 10 min at 50 ^{o}C. The adsorbed CO_2 was probed with vapor phase. HCl using a pippet close to the sample under flowing CO_2 and Ar. The changes in the spectra during batch calibration, CO_2 adsorption/desorption, and HCl vapor treatment were taken in scanning mode with 32 co-added scans and a resolution of 4 cm^{-1} at a rate of 6 scans/min.

4. Results and discussion

4.1. SO_2 adsorption on PEG-400 liquid films

Figure 6 shows the absorbance spectra generated from the adsorption of 260 ppm SO_2 on a PEG-400 thin film. The formation of absorbed species is observed within the first minute of SO_2 exposure suggesting fast adsorption kinetics of SO_2 on PEG-400. Fast adsorption kinetics is a necessary characteristic of a sorbent additive to provide an alternative adsorption site to the amine site; also having shown to rapidly adsorb SO_2. The formation of broad absorption bands in the range of 1000 to 1180 and 3660 to 3190 cm^{-1} indicates a high degree of hydrogen bonding between the oxygen atoms of SO_2 with the hydroxyl groups of PEG-400. The strong intensities generated in the range of 1200 to 1500 cm^{-1} are the result of symmetric and asymmetric vibrations of adsorbed SO_2 species. Another key result of the SO_2 adsorption study over PEG400 is that the intensity of adsorbed species continued to increase throughout the 10 minute adsorption cycle. The continuous increase in absorption intensity indicates that the PEG-400 thin film had not yet reached its maximum adsorption capacity of SO_2. Both results support the hypothesis that addition of PEG-400 to the solid sorbent could provide competitive adsorption sites of SO_2 with the adsorption sites of the amine.

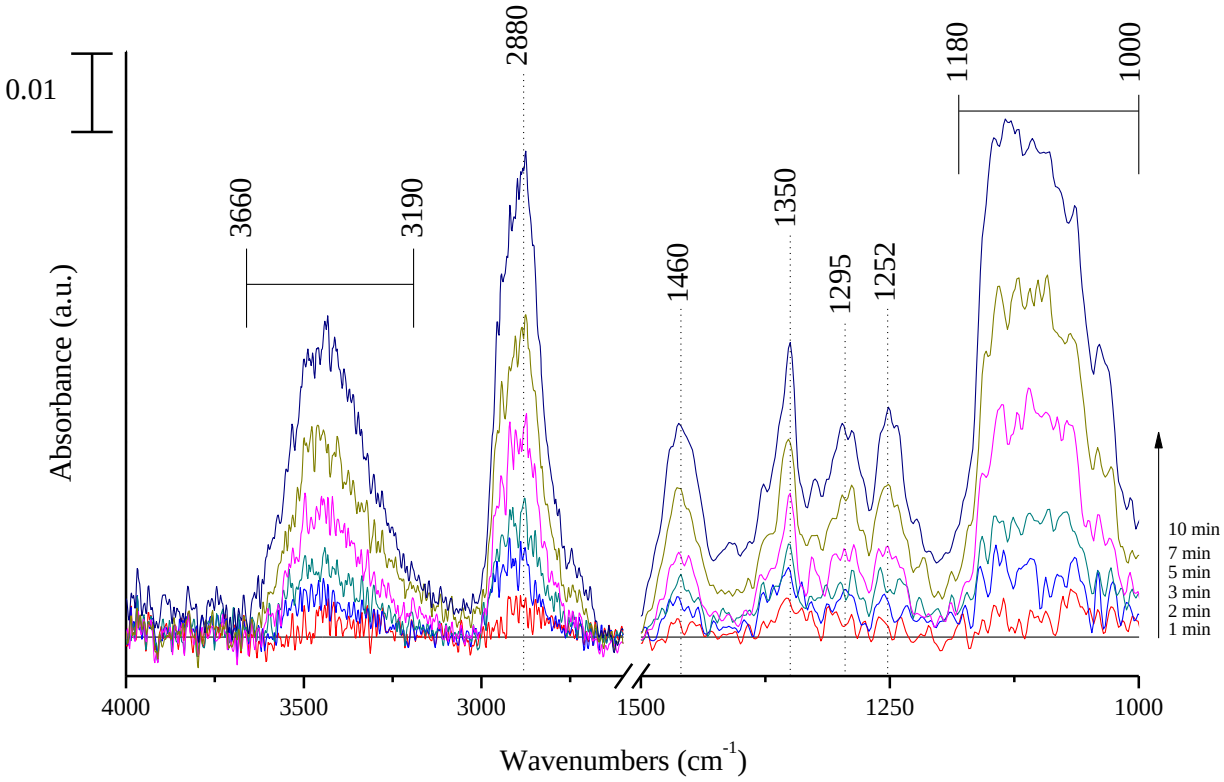

Figure 6: Absorbance spectra of PEG400 thin film showing the formation of SO2 adsorbed species in the presence of 260 ppm SO2 at a flow rate of 50 cm3/min for 10 minutes.

Figure 7 shows the results of the temperature programmed desorption of SO_2 adsorbed species. A small change in the intensity of adsorbed species was observed as the temperature was increased from 40 ^oC to 110 ^oC. This suggests a significant amount of energy is needed to break the strong bond between SO_2 and the PEG film. In fact, a change in the intensity for the adsorbed species was only observed at a temperature greater than 110 ^oC. The absorbance spectrum generated for the TPD temperature of 120 ^oC is nearly flat across the entire FTIR range. The flat spectrum represents the differences between the initial and final states, indicating complete desorption of SO_2 adsorbed species and regeneration of the PEG-400 thin film. The desorption temperature result offers a potential use of PEG-400 in CO_2 capture sorbents, in which the SO_2 adsorbed species are able to be relieved at a different temperature than CO_2 adsorbed species from the sorbent. The solid amine sorbent have shown that CO_2 adsorbed species are able to be desorbed at temperatures in the range of 80-100 ^oC. Since, the desorption temperatures of the two adsorbed species are different, there is potential of applying a two step desorption process. The two step desorption process would occur sequentially at the two temperatures, providing a method for selective desorption of CO_2 and SO_2 adsorbed species.

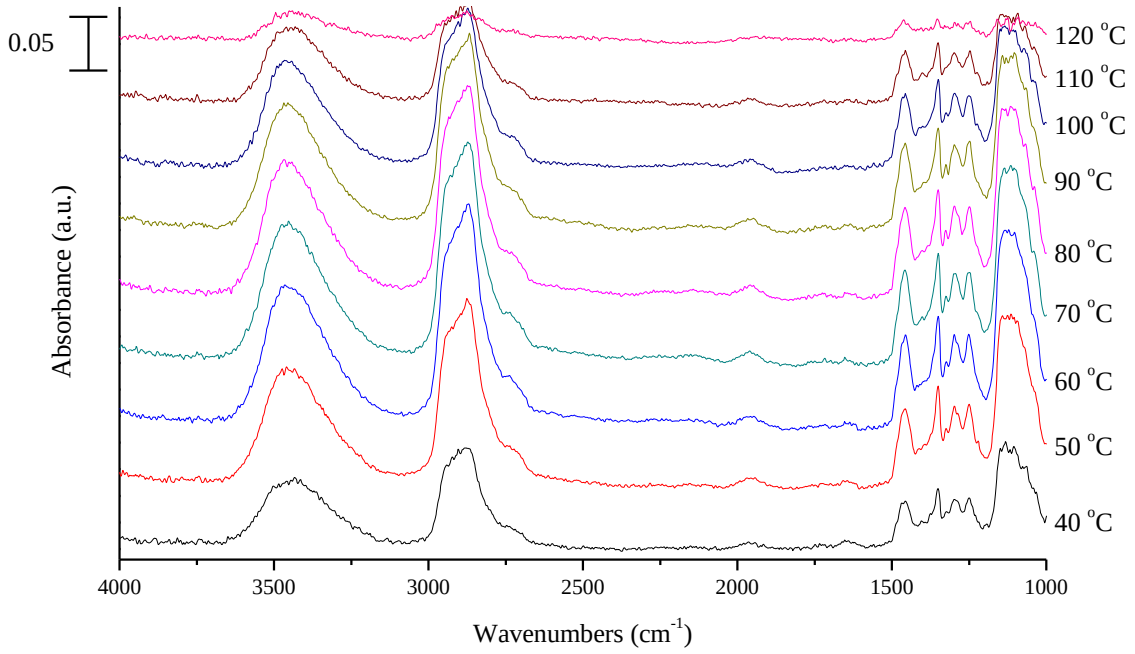

Figure 7. Absorbance spectra at various temperatures of PEG400 film throughout the TPD cycle step.

The PEG-400 thin film was found to readily adsorb SO_2 at 40 ^oC, with nearly complete regeneration at a temperature above that of CO_2 desorption, offering several options are for increasing the SO_2 resistance of our solid amine sorbent. The immediate consideration would be to add an optimized amount of the PEG-400 liquid to the formulation of the solid amine sorbent. The addition of PEG-400 to the solid amine sorbent would provide SO_2 adsorption sites that would compete with the SO_2 adsorption sites of the amine. The optimization would require a time extensive process to find the best combination to maintain a high CO_2 capture capacity while providing SO_2 resistance. A second approach to achieve the two-stage capture and desorption of CO_2 and SO_2 would be making a solid sorbent having only PEG-400. This solid sorbent would be used prior to the amine sorbent in the capture process and solely intended for the removal of SO_2 from the flue gas.

Conclusions:

PEG400 was capable of adsorbing SO_2 at a concentration of 260 ppm balanced in air at 40 ^oC. The liquid film continued to adsorb SO_2 throughout the 10 minute adsorption cycle suggesting a high capture capacity of SO_2. The temperature programmed desorption study confirmed the PEG400 thin film was able to be regenerated at elevated temperatures. The temperature of maximum SO_2 desorption was determined to be greater than 110 ^oC. Since the SO_2 desorption temperature is different than that of CO_2 desorption from the amine, a two step desorption process may be used to selectively desorb the two species from the solid sorbent. It may also be

practical to develop a solid sorbent consisting only of PEG-400 that can be used prior to the amine sorbent in the capture process with the intent of removing the SO_2 gas from the flue gas before it gets to the amine sorbent. In both cases, the addition of PEG-400 would increase the SO_2 resistance of the amine sorbent by providing SO_2 adsorption sites that would compete with those provided by the amine.

4.2. Effect of PEG on SO_2 adsorption of TEPA liquid films

Mass spectrometric studies of SO_2 adsorption/desorption on TEPA/PEG films

Figure 8 shows the SO_2 MS profile of the first SO_2 capture cycle on TEPA/PEG (1:2) film. The MS profile of SO_2 shows that step-switch was achieved by 4-port valve which gives a smooth switch of gas from N_2 at 100 cm^3/ min to SO_2 30 cm^3/min. Flowing SO_2 over the TEPA/PEG (1:2) thin film increased the SO_2-MS intensity and attained a steady state after 7 min of adsorption. The film was saturated with SO_2 for 30 min and purged by N_2 flow of 100 cm^3/min for 20 min to remove the gas phase SO_2. Four 3 cm^3 pulses of pure SO_2 are introduced by 6 port valve for calibration. The SO_2 MS profile during TPD was magnified. The circles with notations i-iv on the MS profile represent the points at which the IR spectra of the films are considered to determine the type of species present on the film. Figure 3 shows the SO_2 MS profiles during TPD for the first cycles of pure TEPA, TEPA/PEG (2:1), TEPA/PEG (1:1), TEPA/PEG (1:2) and pure PEG thin films. The SO_2 started to desorb as soon as temperature was increased and reached the maximum (T_{max}) between 90-100 ^oC. The area under desorption peaks for pure TEPA and PEG are negligible compared to those with TEPA/PEG films. Figure 9 also shows increase in the peak area of SO_2 and decrease in the T_{max} of desorption with increase in the PEG composition in the films. Table 2 shows the T_{max} of desorption and SO_2 capture capacity for 3 cycles on the thin films. Pure TEPA and PEG showed very negligible capture capacities of 18.4 µmol/µmol TEPA and 14.4 µmol/µmol PEG respectively. The addition of PEG to TEPA has increased the capture capacities of the thin films by 80 folds and increase in the order TEPA/PEG (2:1) < TEPA/PEG (1:1) < TEPA/PEG (1:2). The SO_2 capture capacities, T_{max} and (%) degradation of the films over 3 cycles are presented in Table 2. The results in table 2 show that the SO_2 capture capacities of the films increased drastically by mixing TEPA and PEG. The (%) degradation of the films was also decreased in TEPA/PEG mixture with increase in PEG composition of the film. These results show that the mixture of TEPA/PEG can capture SO_2 better than TEPA and PEG in their pure forms. The reasons for the increase in SO_2 capture capacities and stability of the films are further investigated by ATR-IR.

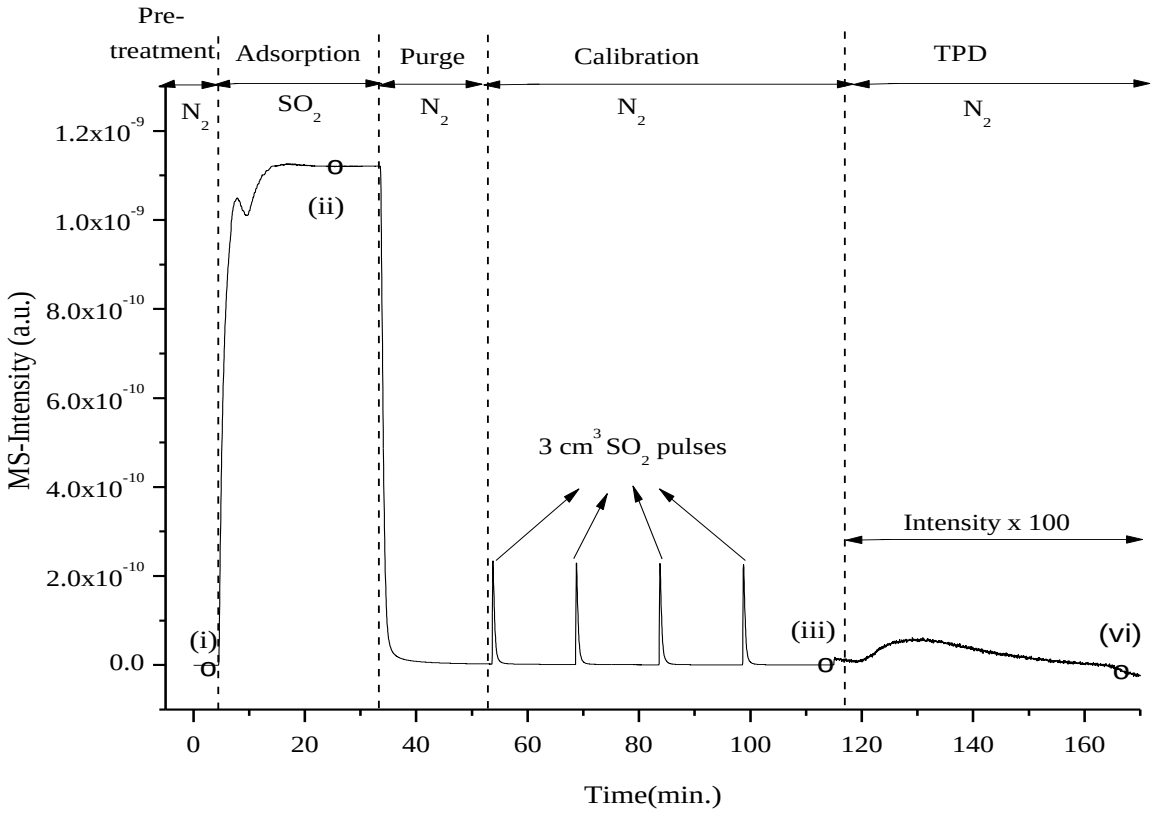

Figure 8: SO_2 MS profile during the 1st cycle over TEPA/PEG (1:2) thin film

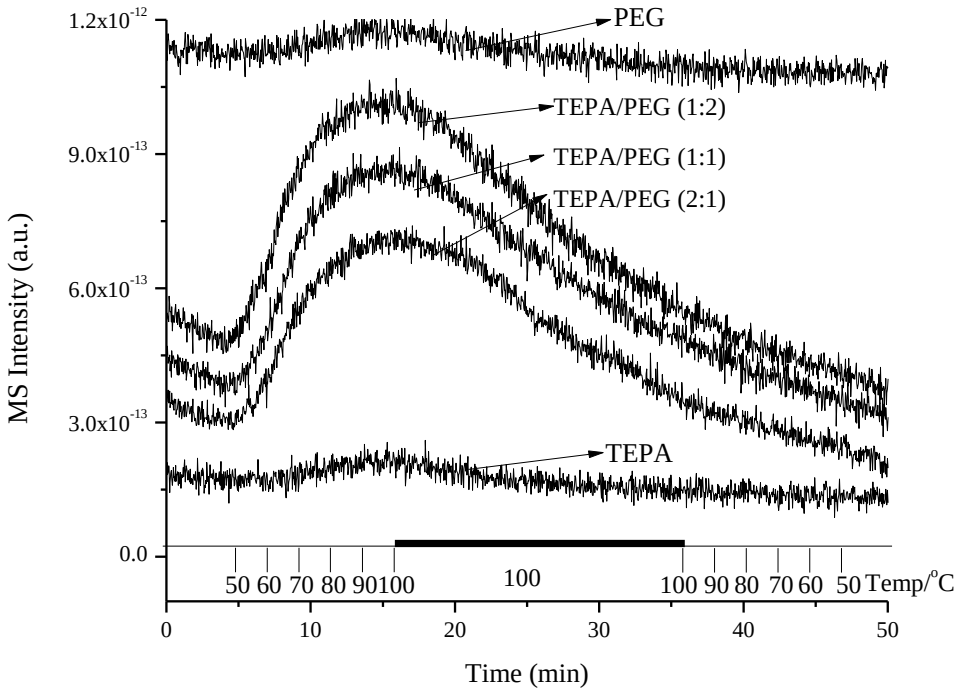

Figure 9: SO_2 MS profile during TPD of 1st cycle of TEPA/PEG (2:1), TEPA/PEG (1:1), TEPA/PEG (1:2) thin films

Table 2: SO_2 capture capacities and T_{max} of desorption and % degradation on TEPA/PEG films for 3 cycles

TEPA/PEG composition	Tmax (^oC) (Average)	SO_2 capture (µmol/µmol TEPA) Cycle 1	Cycle 2	Cycle 3	% Degradation
TEPA	100	18.4	13.7	12.0	34.7
2:1	100±0.5[a]	830	580	170	79.5
1:1	97±0.5	980	780	810	17.4
1:2	94±0.5	1150	1050	1060	7.9
PEG	100	14.4	12.7	10.6	26.3

[a] average for two cycles. For third cycle the Tmax was only 65 ^oC as only small amount of SO_2 desorbed

ATR-IR Results

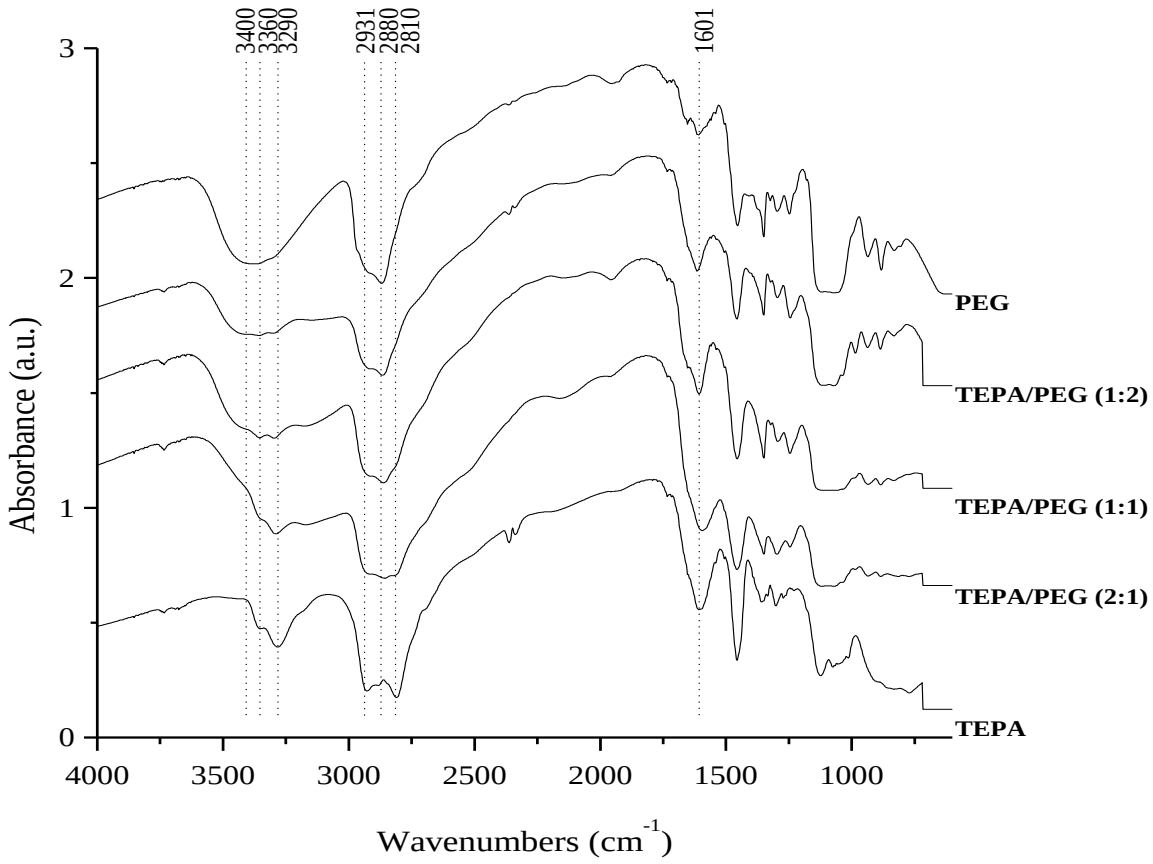

Figure 10: ATR-IR single beam spectra of fresh TEPA, TEPA/PEG and PEG-200 films.

Figure 10 show the ATR-IR single beam spectra of fresh TEPA, TEPA/PEG and PEG thin films prior to SO_2 adsorption study. The IR spectra of TEPA show characteristic bands at 3360 and 3290 cm^{-1} for asymmetric and symmetric stretching of NH_2, 1601 cm^{-1} for deformation of amine and bands at 2810, 2880 and 2931 cm^{-1} for C-H stretching. The IR band assignments in the present study are showed in Table 3. The spectra of TEPA/PEG (2:1), (1:1) and (1:2) show the development of broader amine bands between 3700-3000 cm^{-1}. The formation of broad amine bands in the films was attributed to the formation of hydrogen bonding between (NH_2/NH) groups of TEPA and OH groups of PEG. The broadening of amine bands increased with the PEG composition of the film. The IR single beam spectra of PEG show a broad band between 3700-3000 cm^{-1} due to hydrogen bonded OH groups of PEG. The results also suggest the formation of homogeneous mixture of TEPA and PEG on the ATR.

Table 3: IR band assignments

Wave number (cm^{-1})	Assignment	Species	Ref.
3700-3000	hydrogen bonding	PEG, TEPA	6-9
3500-3300	O-H stretching	PEG	10
3290	N-H stretching	TEPA	11-18
3360	N-H stretching	TEPA	11-18
2880	C-H stretching	TEPA, PEG	7,11-13,16-17
2931	C-H stretching	TEPA, PEG	7,11-13,16-17
1643, 1510	N-O stretching	O_2S-**O-N**	19
1320,1360, 1170	Stretching vibrations	SO_2	20-21
1250,1200	S=O stretching	sulfates, sulfites	19,22
1025,1149, 976	S=O stretching	bisulfate, sulfate	22

Pure TEPA

Figure 11 show the ATR-IR absorbance spectra of TEPA film for SO_2 adsorption and TPD for 3 cycles. The spectra for the film showed decrease in the intensities of IR bands at 3360, 3390 cm^{-1} for symmetric and asymmetric vibration of NH_2 and 2931, 2880 and 2810 for symmetric and asymmetric stretching of CH_2 due to adsorption of SO_2. The spectra's also showed formation of broad band in the range 2200-3000 cm^{-1} centered at 2700 cm^{-1} due to hydrogen bonding between adsorbed SO_2 and amines. Adsorptions of SO_2 also showed the formation of IR bands at 1621, 1507, 1320, 1240, 1150, 1149, 976, 900 and 690 cm^{-1}. The strong bands at 1360, 1320, and 1170 cm^{-1} are assigned to stretching vibrations of gas phase and adsorbed SO_2 [21]. The bands at 1200 and 1245 cm^{-1} are assigned to asymmetric and symmetric stretching of sulfites[19]. The bands at 1025, 1149 and 976 cm^{-1} are assigned to stretching vibrations of bisulfate or sulfates[22] and 1621 and 1510 cm^{-1} for N-O stretching[19]. The TPD of the TEPA thin films does not regenerate the amine sites suggesting the strong bond formation between TEPA and SO_2, which is in good agreement with MS results in Table 2. The spectra of the film did not change much after first adsorption and desorption except showing the formation of SO_2 peak during adsorption. Thus the ATR-IR spectra suggest that the SO_2 is strong interaction with TEPA and may require high temperatures for the desorption.

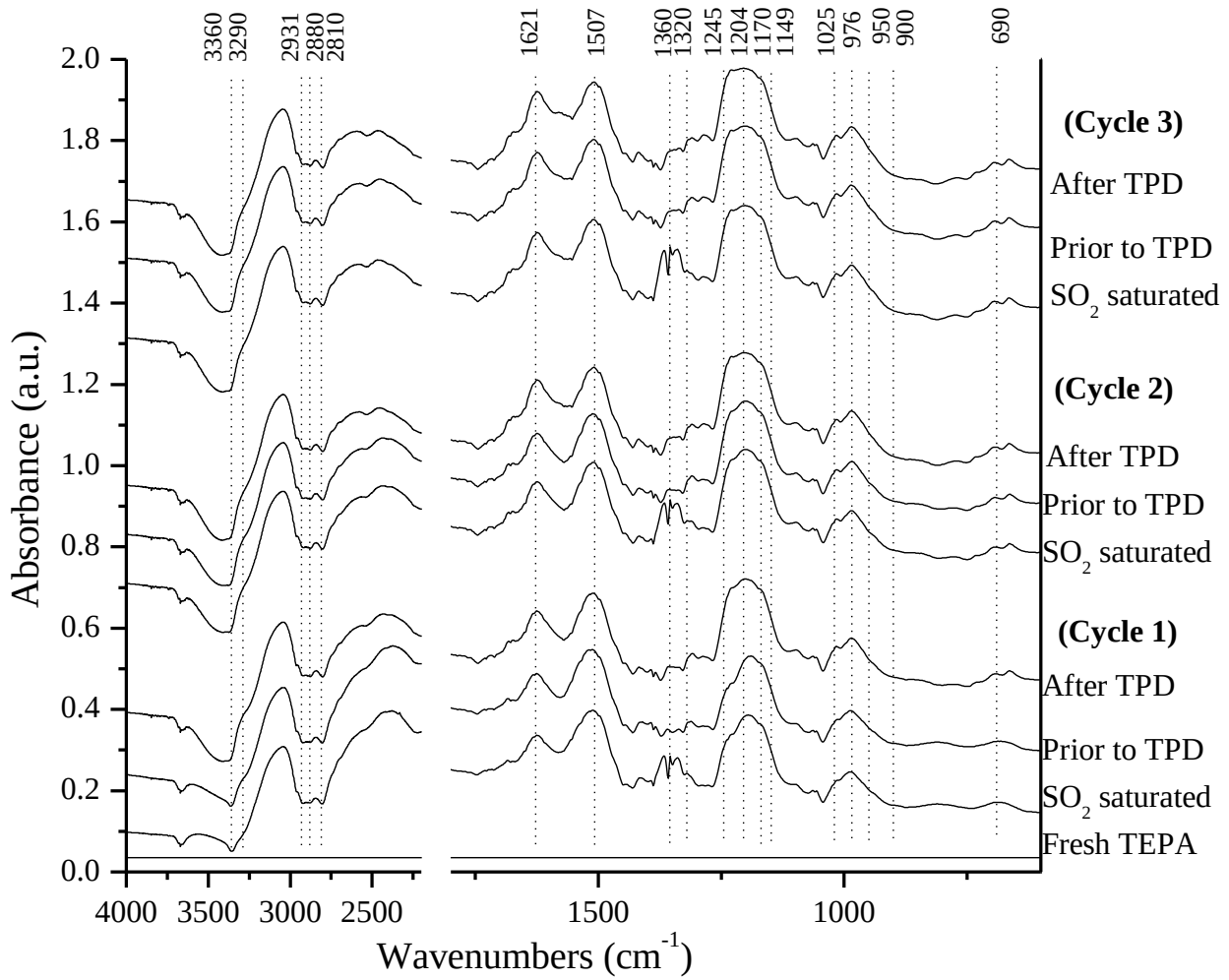

Figure 11: ATR-IR absorbance spectra of pure TEPA film during SO_2 adsorption and TPD for three cycles. Abs=-log(I/I_0) where I is the single beam spectra taken during SO_2 saturation and I_0 the single beam spectra of fresh film prior to any SO_2 adsorption

Pure PEG

Figure 12 show the IR absorbance spectra on PEG film for SO_2 adsorption and TPD for 3 cycles. The spectra show the formation of strong peak at 1325 and 1170 cm^{-1} for the asymmetric stretching band of SO_2 and strong peak at 3550 due to breaking of hydrogen bonding between OH groups of PEG due to SO_2 adsorption. The IR bands at 1245 and 1204 cm^{-1} are due to the S=O stretching vibrations of sulfites. The spectra of the film after TPD show the maximum regeneration of hydrogen bonding of OH groups of PEG thin film. In the second and third cycles the adsorption of SO_2 does not generate peak at 3550 cm^{-1} suggesting poor adsorption of SO_2 on the film in second and third cycles.

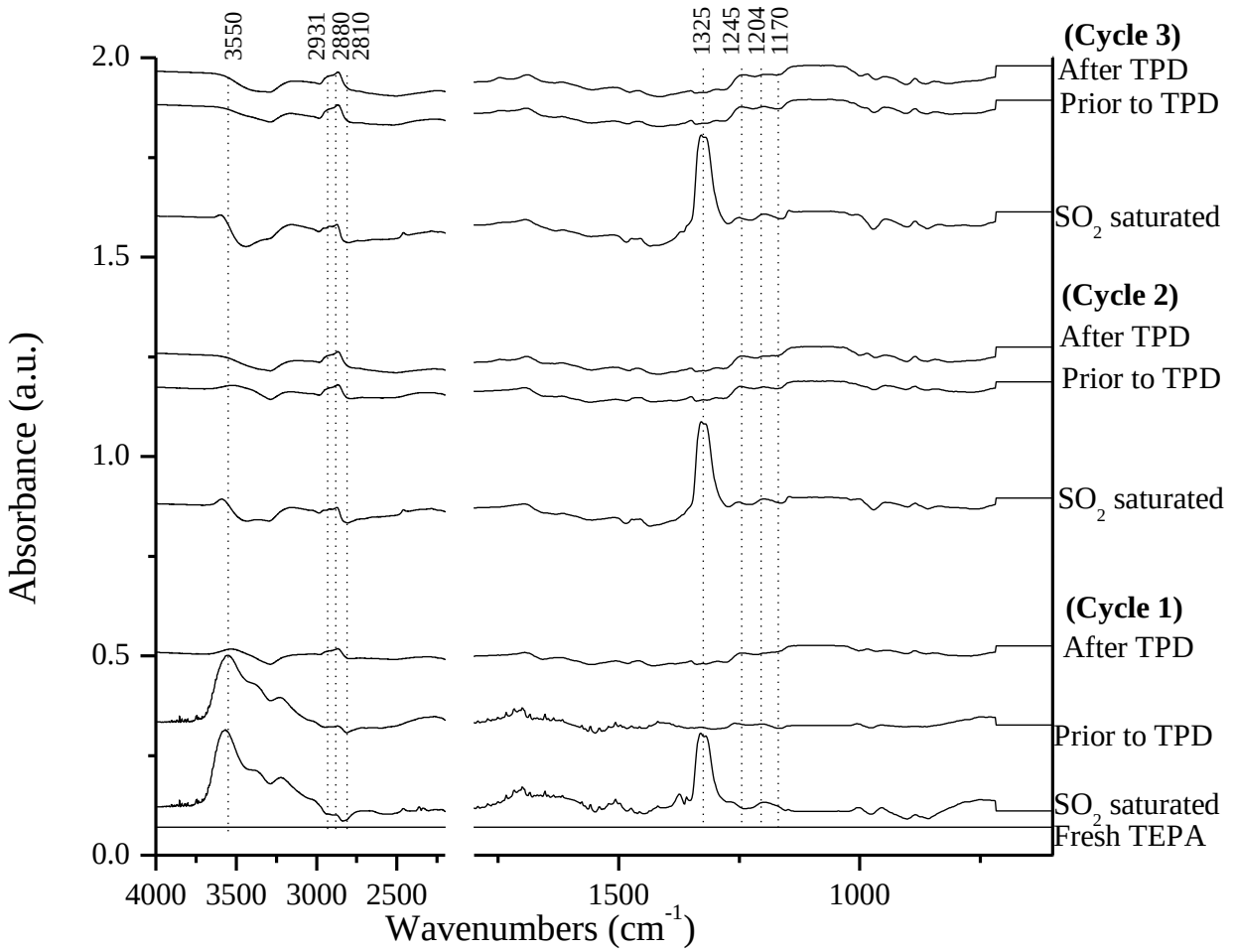

Figure 12: ATR-IR absorbance spectra of pure PEG film during SO2 adsorption and TPD for three cycles. Abs=-log(I/I0) where I is the single beam spectra taken during SO2 saturation and I0 the single beam spectra of fresh film prior to any SO2 adsorption

TEPA/PEG mixtures

Figure 13 show the ATR-IR absorbance spectra for the three cycles with fresh and saturated SO_2 on TEPA/PEG (2:1), TEPA/PEG (1:1) and TEPA/PEG (1:2) thin films. The spectra's for the three films showed decrease in the intensities of IR bands at 3360, 3390 cm^{-1} for symmetric and asymmetric vibration of NH_2 and 2931, 2880 and 2810 for symmetric and asymmetric stretching of CH_2 due to adsorption of SO_2. The spectra's also showed formation of broad band in the range 2200-3000 cm^{-1} centered at 2700 cm^{-1} due to hydrogen bonding between adsorbed SO_2 and amines. Adsorptions of SO_2 also showed the formation of IR bands at 1643, 1320, 1240, 1150, 1149, 976, 900 and 690 cm^{-1}. The strong bands at 1360, 1320, and 1170 cm^{-1} are assigned to stretching vibrations of gas phase and adsorbed SO_2[21]. The bands at 1200 and 1245 cm^{-1} are assigned to asymmetric and symmetric stretching of sulfites[19]. The bands at 1025, 1149 and 976 cm^{-1} are assigned to stretching vibrations of bisulfate or sulfates[22] and 1643 cm^{-1} for N-

O stretching[19]. Increasing the PEG compositions in the films showed increase in S=O stretching of sulfates at 1149 and 976 cm^{-1} with decrease in bisulfate's at 1245, 1204 cm^{-1} and N-O stretching at 1643 cm^{-1}. TEPA/PEG (2:1) film with low PEG composition shows distinct peaks at 976, 1025 and 1050 cm^{-1} for bisulfate's decreased with increasing PEG compositions. The sharp decrease in the intensity of amines at 3360 and 3390 cm^{-1} with increase in PEG compositions suggest that presence of large amount of PEG enhances the SO_2 adsorption capacity of the films through interaction with the NH_2 functional group.

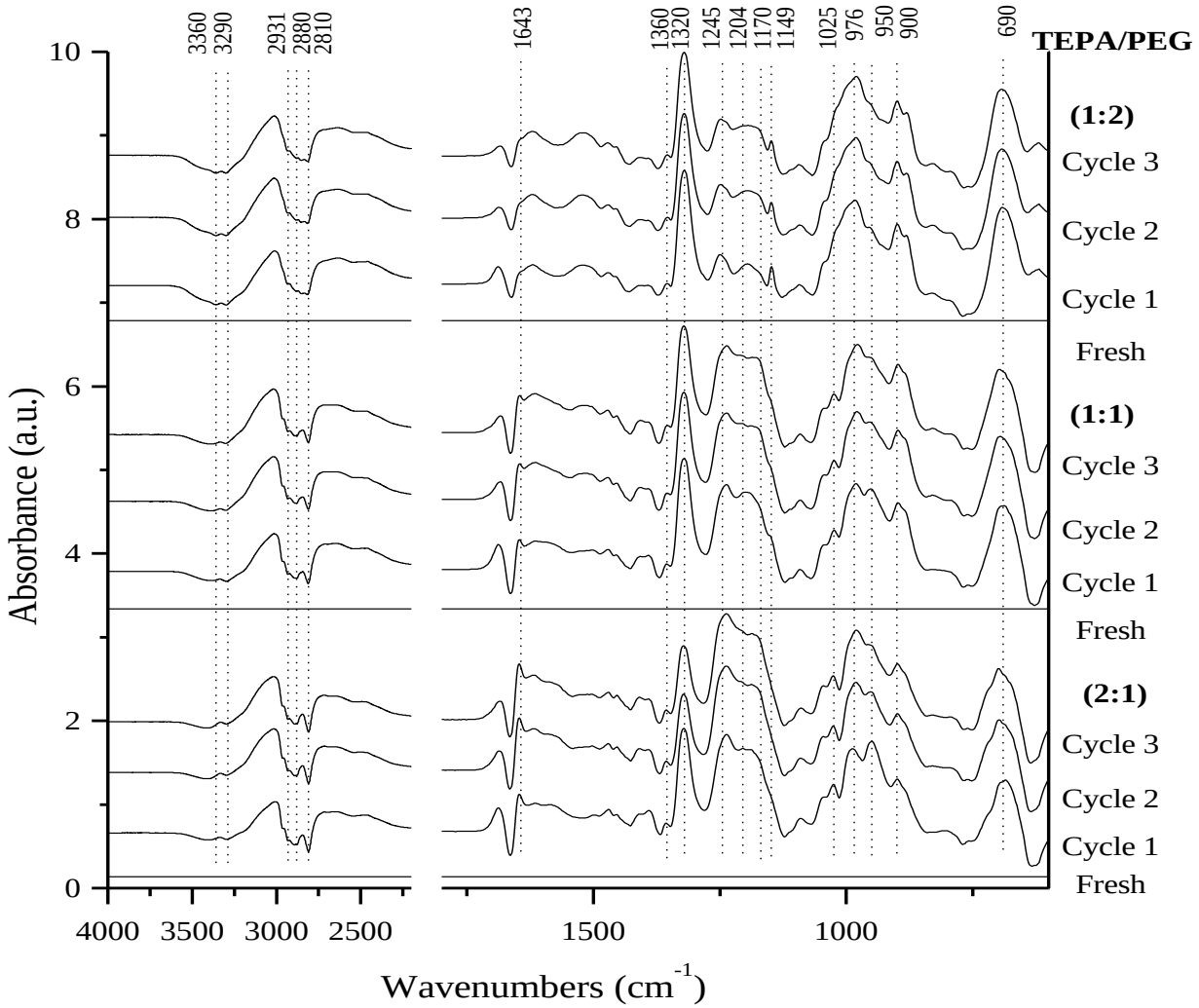

Figure 13: ATR-IR absorbance spectra on TEPA/PEG films with SO2 saturation for three cycles. Abs=-log(I/I0) where I is the single beam spectra taken during SO2 saturation and I0 the single beam spectra of fresh film prior to any SO2 adsorption

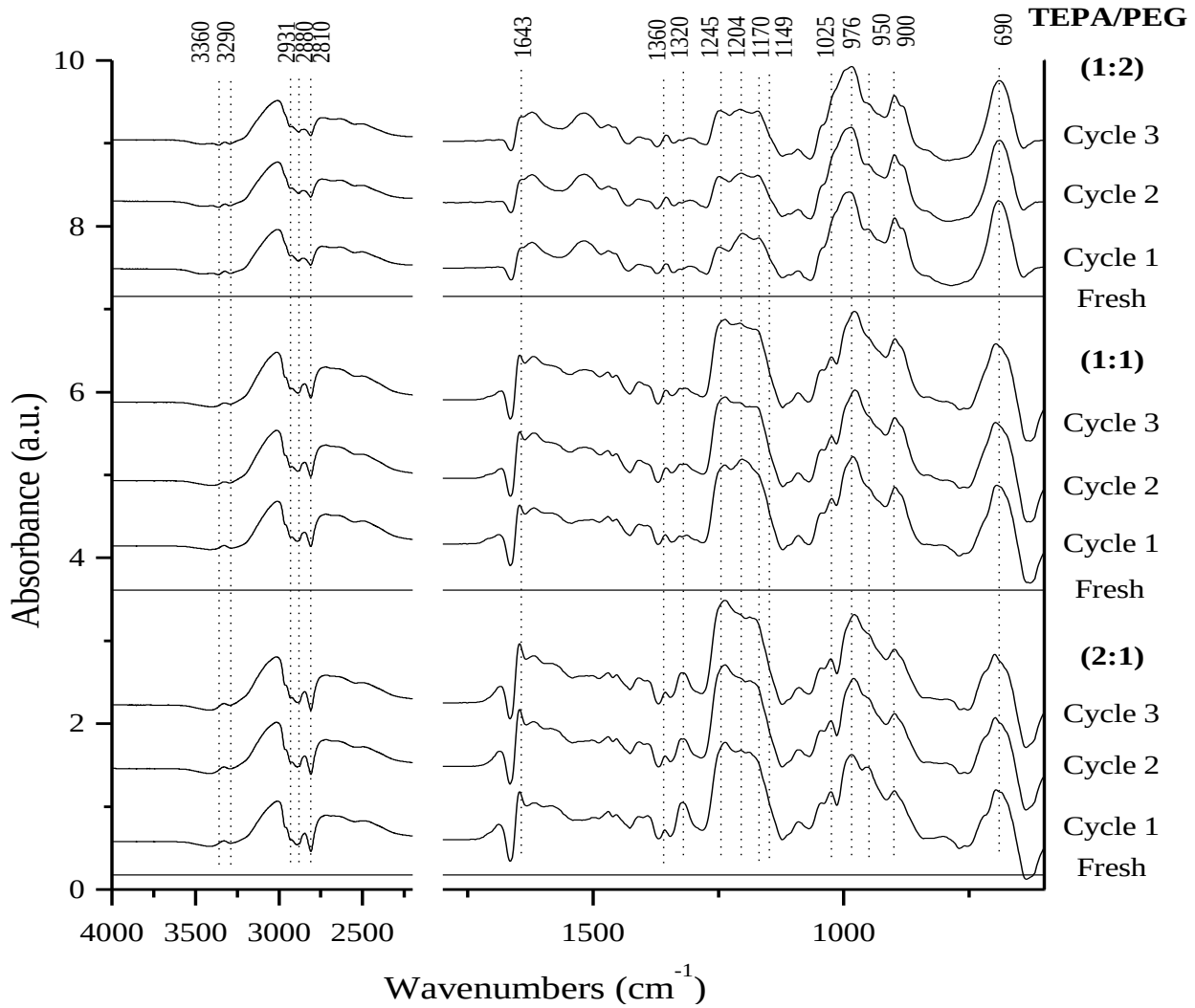

Figure 14: ATR-IR absorbance spectra on the TEPA/PEG thin films after N_2 flushing. Abs=-log(I/I_0) where I is the single beam spectra taken after N_2 flushing and I_0 the single beam spectra of fresh film prior to any SO_2 adsorption

The thin films are purged under N_2 flow at 100 cm^3/min for 20 min after SO_2 saturation. N_2 flushing was carried out to remove the weakly adsorbed SO_2 from the thin films. Figure 8 show the ATR-IR absorbance spectra for the three cycles on TEPA/PEG (2:1), TEPA/PEG (1:1) and TEPA/PEG (1:2) thin films after N_2 flushing. *The spectra showed a decrease in intensity of gas phase SO_2 at 1320 cm^{-1} a slight increase in intensity of S=O stretching of adsorbed SO_2 at 1360 and 1170 cm^{-1}*. The band at 1150 cm^{-1} in TEPA/PEG (1:2) is completely disappeared suggesting the weaker interaction of SO_2 on the films with more PEG. The intensities of IR bands at 3360 and 3290 cm^{-1} for amines are strong in the TEPA/PEG (2:1) and decreased with increasing concentration of PEG in the films. This suggests the strong interactions of SO_2 with films containing less PEG. The strong interactions of SO_2 with amines required high temperatures for desorption, which is evident from the TPD profiles in Figure 10. TPD-MS profiles showed that

the T_{max} of desorption decreased and the amount of SO_2 desorbed increased with increase in the PEG composition of the film. This suggests that the results from IR and MS are in good agreement with each other.

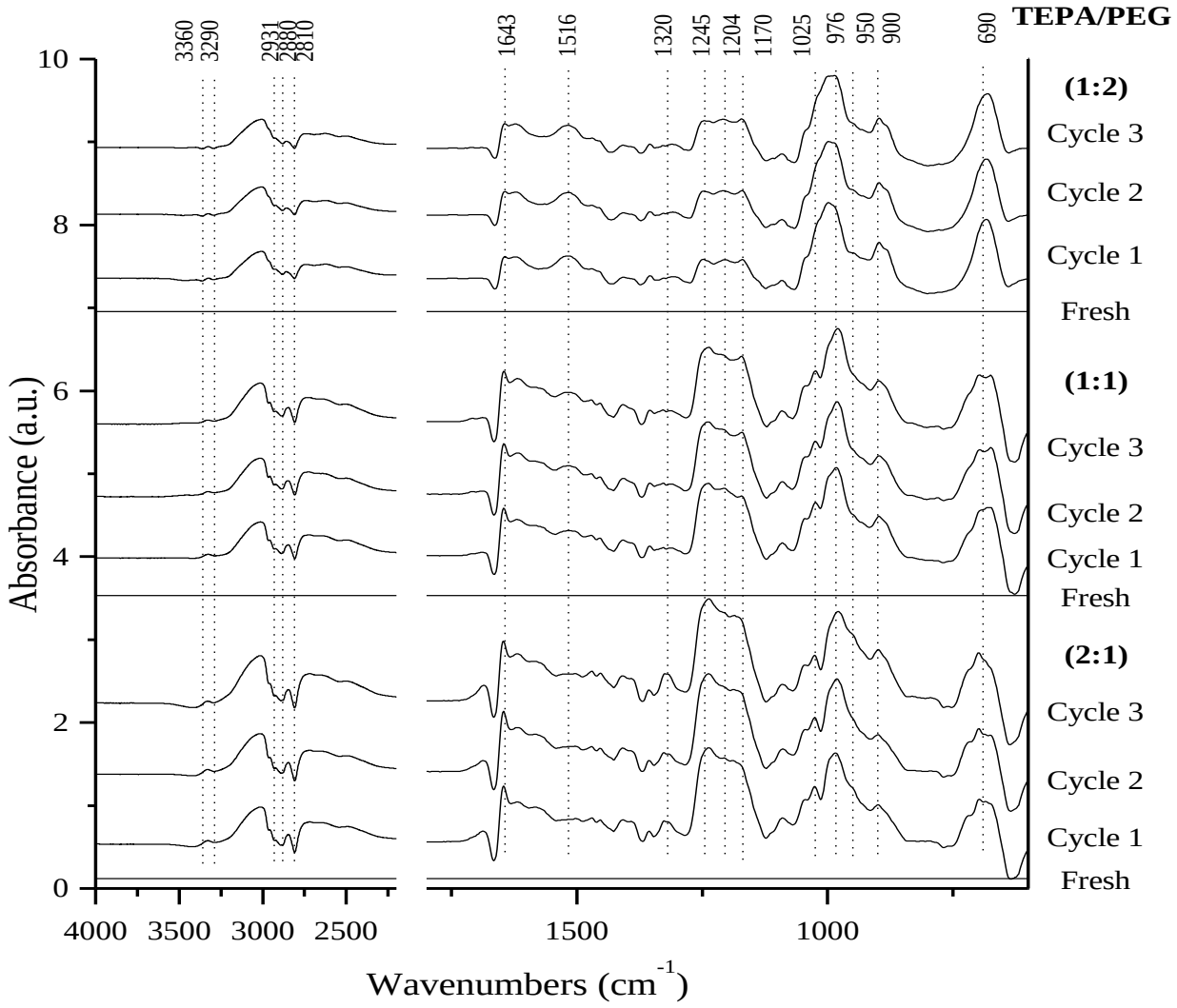

Figure 15: ATR-IR absorbance spectra on the TEPA/PEG thin films after TPD. Abs=-log(I/I_0) where I is the single beam spectra taken after TPD flushing and I_0 the single beam spectra of fresh film prior to any SO_2 adsorption

Figure 15 show the ATR-IR absorbance spectra for the three cycles of fresh and after TPD profiles of TEPA/PEG (2:1), TEPA/PEG (1:1) and TEPA/PEG (1:2) thin films. The spectra for TEPA/PEG (1:2) showed maximum retention of amine bands at 3360 and 3290 cm^{-1} suggesting almost complete SO_2 desorption from the films. The spectra's of TEPA/PEG (2:1) and TEPA/PEG (1:1) films showed that the intensities of amines due to strongly adsorbed SO_2 indicating that after TPD large amount of SO_2 still was remained on the films. This is also evident from the IR bands at 1245, 1204 and 1170 cm^{-1}. The intensities of these bands are stronger in TEPA/PEG (2:1) film with less PEG than those of TEPA/PEG (1:2). These results

are in agreement with the results of TPD-MS where TEPA/PEG (1:2) show higher amount of SO_2 desorbed than TEPA/PEG (2:1). The presence of strongly adsorbed SO_2 species on the TEPA/PEG (2:1) films blocks the amine sites for further adsorption of SO_2 in second and third cycles. Hence, the decreases in the SO_2 capture capacities of the TEPA/PEG (2:1) in the second and third cycles are attributed to the strongly adsorbed SO_2. Increase in PEG compositions of the films also increased the SO_2 capture capacities of the films which is evident from the MS results in Table 2. The increase in PEG compositions also decreases the SO_2-amine interaction allowing maximum desorption of SO_2 during TPD which in turn gives more number of amines sites available for re-adsorption in second and third cycles. The increase in PEG compositions also decreased SO_2-amine interaction which in turn decreased the T_{max} required for desorption as revealed from TPD-MS profiles in Figure 3. The increase in the stability of the thin films with PEG composition is attributed decrease in the SO_2-amine interaction which favors desorption of SO_2 during TPD.

Conclusions

SO_2 adsorption and desorption on TEPA/PEG thin films was investigated by in-situ ATR-IR and MS. The MS results showed that pure TEPA or PEG possess very poor SO_2 capture capacities. However, the mixture of TEPA and PEG showed high capture capacities. The presence of PEG improved the capture capacities and stability of the film. ATR-IR single beam spectra of the films showed that increasing the PEG concentration in the TEPA/PEG film increased hydrogen bonding between NH_2/NH groups of TEPA and OH groups of PEG. ATR-IR absorbance spectra during SO_2 adsorption showed stronger decrease in the amines peak intensities in TEPA/PEG films with high PEG composition suggesting high availability of amines sites for SO_2 the capture. The IR absorbance spectra after TPD on the TEPA/PEG films showed strongly adsorbed SO_2 in the films with less PEG. The increase in PEG concentration also decreased the SO_2-amine interaction which further decreased the T_{max} required for desorption. The high stability of the TEPA/PEG (1:2) film is attributed decrease in the strength of SO_2-amine interaction with increasing amounts of PEG in the film.

4.3. Effect of H_2O on SO_2 adsorption of TEPA liquid films

Figure 16 shows the IR absorbance spectra of fresh TEPA and TEPA/H_2O thin films prior to SO_2 adsorption. The IR spectrum of TEPA shows characteristic bands at 3360 and 3290 cm^{-1} for asymmetric and symmetric stretching of NH_2, 1600 cm^{-1} for deformation of amine and bands at 2815 and 2940 cm^{-1} for C-H stretching. The spectra of TEPA/H_2O solutions containing 30 and 50 w% TEPA show that the presence of water broadened the bands for amine stretching at 3360 and 3290 cm^{-1} and the bending vibrations at 1600 cm^{-1} as a result of hydrogen bonding formation between water and amine groups of TEPA. The broadening of amine bands increased with

increase in water content in the thin film. The decrease in intensity of the NH_2 and CH_2 bands in water containing films can be attributed to the decrease in TEPA composition in the film.

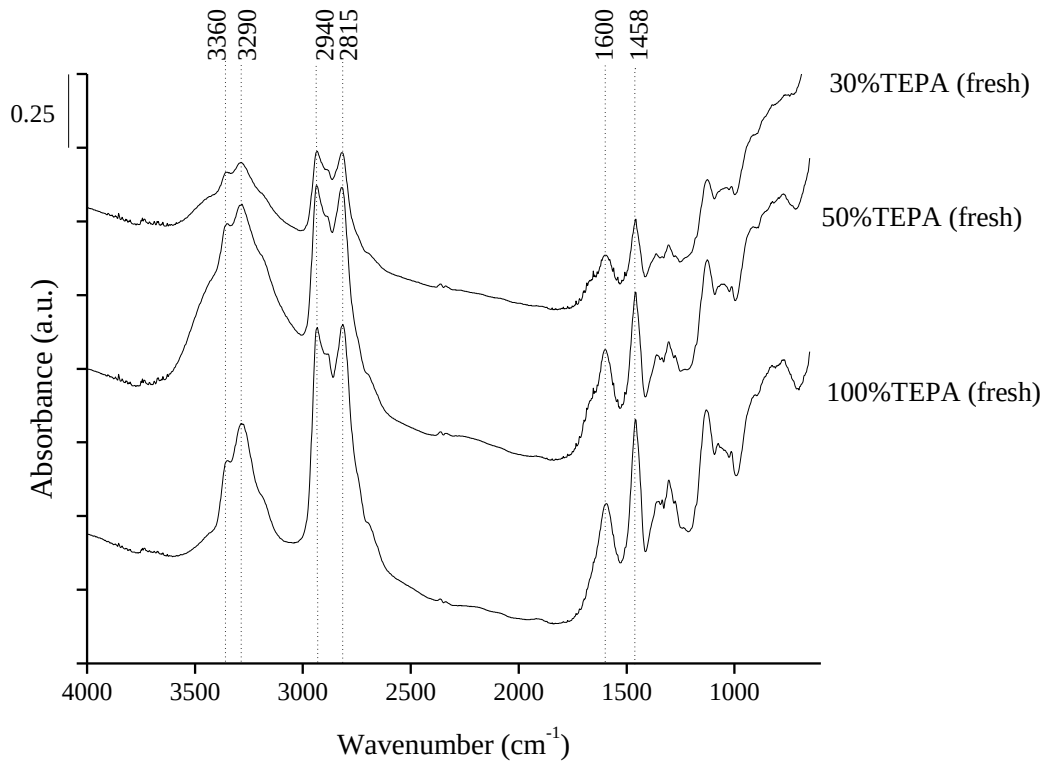

Figure 16: IR absorbance spectra of fresh TEPA and TEPA/H2O thin films.

Figure 17 shows the IR absorbance spectra of the TEPA film with adsorbed SO_2, after Ar purge, and the spectral changes of the film with adsorbed SO_2 during the temperature programmed desorption (TPD). The spectrum of the film after SO_2 adsorption shows a decrease in the intensity of amine bands at 3360 and 3290 cm^{-1} and the decrease of C-H bands at 2815 and 2940 cm^{-1}. The spectrum shows strong bands at 3000, 1635 and 1530 cm^{-1} for NH_3^+ ion formation[1] and a broad peak centered at 2275 cm^{-1} for the hydrogen bonding between adsorbed SO_2 and amines. The band at 1370 cm^{-1} represents gas phase SO_2.[2-3] The adsorption of SO_2 produced strong and broad band centered at 970 cm^{-1} for S-O stretching in sulfite (SO_3^{2-}) and weak absorptions at 1185 cm^{-1} for S=O stretching in bisulfate ($S_2O_5^{2-}$). The formation of sulfite or bisulfate requires two ammonium ions i.e., 4 NH_2 sites for their adsorption. Switching the DRIFT cell to continuous mode under flowing Ar removed the gas phase SO_2 from the DRIFTS cell, which is evidenced by the decrease in intensity of 1370 cm^{-1}. TPD on the adsorbed SO_2 on TEPA film decreased the intensity at 970 cm^{-1} of S-O stretching of sulfite and increased the intensity of bands at 1185 and 1245 cm^{-1} for bisulfate and chemisorbed SO_2. TPD also produced additional bands at 1094 and 10 31 cm^{-1} which are assigned for sulfate (SO_4^{2-}). The results

indicate that SO_2 is strongly adsorbed on TEPA and inter-conversion to different adsorbed SO_2 species occur when heat treatment is applied to the samples.

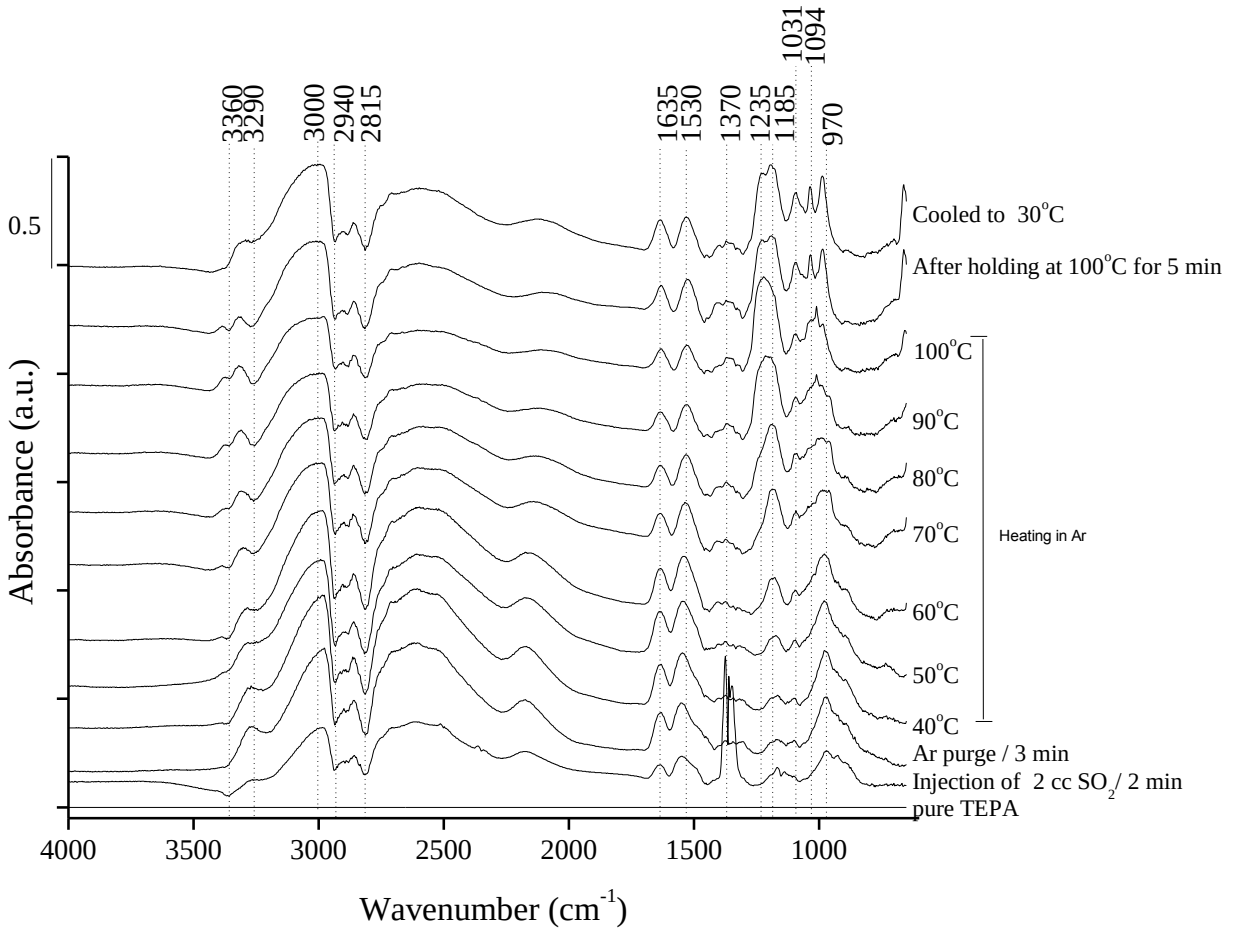

Figure 17: IR absorbance spectra of SO2 adsorption and desorption on pure TEPA thin film on metal cup.

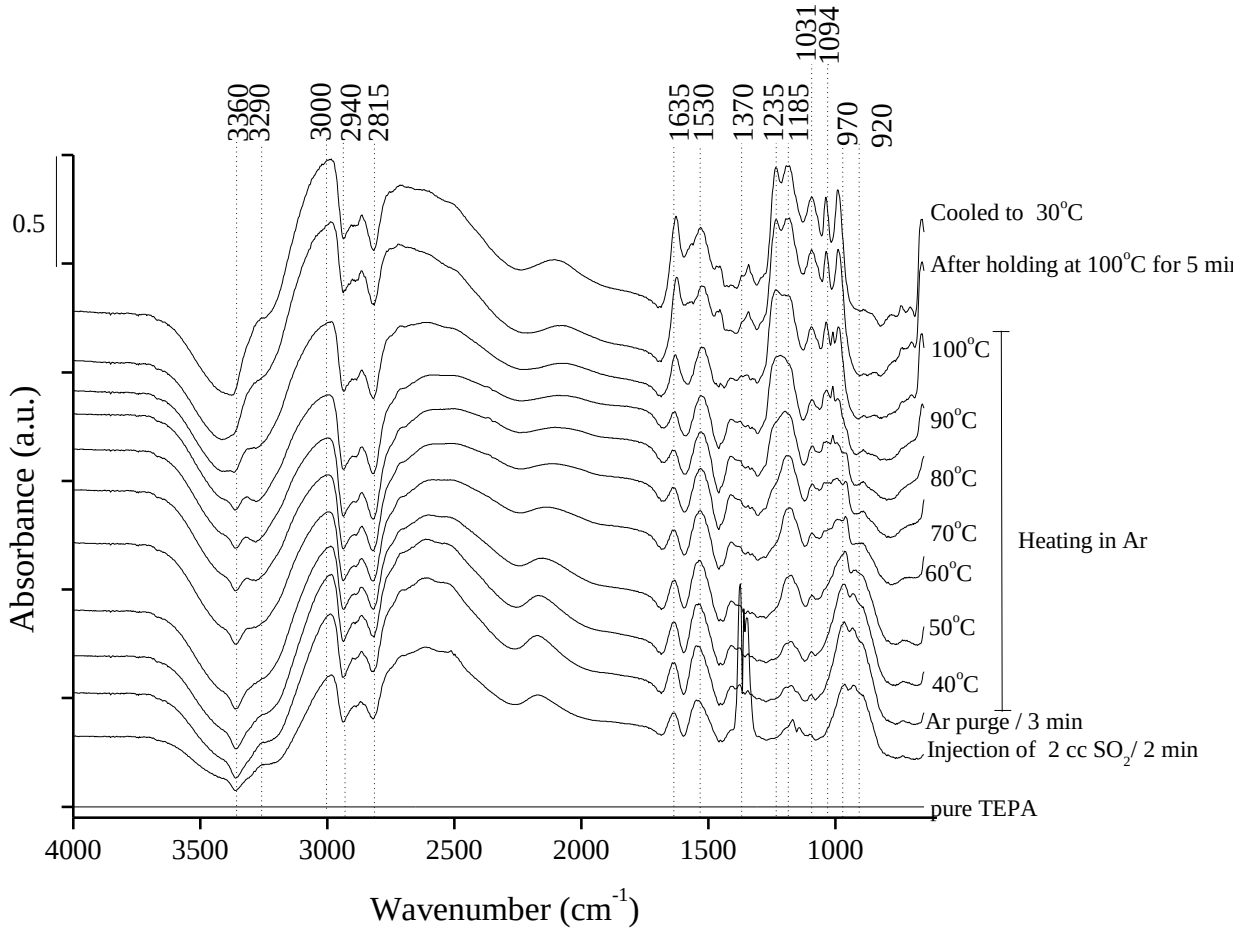

Figure 18: IR absorbance spectra of SO_2 adsorption and desorption on TEPA/H_2O 50/50 thin film on metal cup.

Figure 18 shows the IR absorbance spectra of the TEPA/H_2O 50/50 thin film with adsorbed SO_2, after Ar purge, and the spectra changes on adsorbed SO_2 during temperature programmed desorption (TPD). The spectrum of the TEPA/H_2O film with adsorbed SO_2 shows a broad decrease in the intensity of amines due to the breaking of hydrogen bonding between TEPA and water during SO_2 adsorption. This spectrum also shows a band for NH_3^+ ion formation, and the hydrogen bonding between adsorbed SO_2 and amines similar to that observed on the TEPA thin film. The presence of water in TEPA thin film increased the intensity of the broad band centered at 970 cm^{-1} for S-O stretching in sulfite (SO_3^{2-}) and produced an additional band at 920 cm^{-1} for dative bonding formation between amine and SO_2. The adsorption of SO_2 through dative bonding requires only one amine site per SO_2 showing increased SO_2 adsorption capacity compared to pure TEPA. The increase in SO_2 adsorption via dative bonding can be attributed to the increase in the distance between TEPA molecules in the presence of water. Switching the gas from SO_2 to Ar removed the gas phase SO_2 from the DRIFTS cell which is evidenced by the decrease in intensity of 1370 cm^{-1}. TPD on the thin film decreased the intensity at 970 cm^{-1} of S-O stretching by reaching 90 ^oC suggesting desorption of adsorbed SO_2 from the film. This

clearly indicates that the presence of water in the TEPA film decreased some of the SO_2-amine interactions. However, after reaching a temperature of 100 ^oC, the transformation of sulfite to sulfate species is observed. This observation can be attributed to the evaporation of water which increases the strength of the SO_2-amine interactions and inter converts the adsorbed species to those observed on pure TEPA thin film.

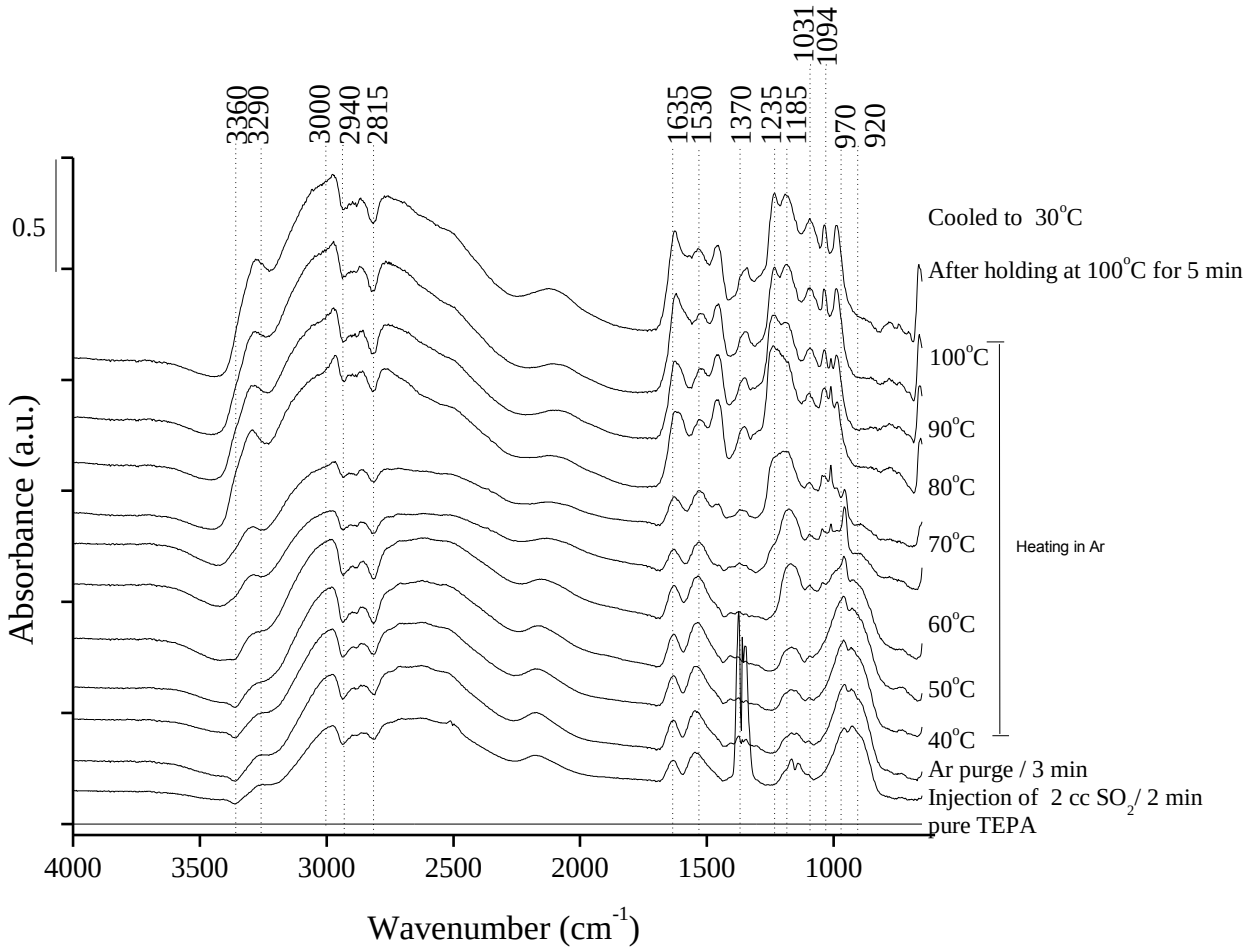

Figure 19: IR absorbance spectra of SO_2 adsorption and desorption on TEPA/H_2O 30/70 thin film on metal cup.

Figure 19 shows the IR absorbance spectra of the TEPA/H_2O 30/70 thin film with adsorbed SO_2, after Ar purge, and the spectra changes on adsorbed SO_2 during temperature programmed desorption (TPD) on TEPA/H_2O 30/70 thin film. The spectrum of the TEPA/H_2O 30/70 thin film with adsorbed SO_2 shows further broadening of amine stretching after SO_2 adsorption. The spectrum also shows the band for NH_3^+ ion formation and the hydrogen bonding between adsorbed SO_2 and amines similar to that observed on pure TEPA thin film. The intensity of the broad band centered at 970 cm^{-1} for S-O stretching in sulfite (SO_3^{2-}) and dative bonding between amine and SO_2 did not show much variation in the intensity with increase in water content of the sample. This can be attributed to the overall decrease in the amine content in the sample. TPD

on the thin film decreased the intensity at 970 cm^{-1} of S-O stretching at temperatures around 70 ^{o}C, suggesting desorption of adsorbed SO_2 from the film. This clearly indicates that increasing the water content in the sample decreases SO_2-amine interactions and reduced the desorption temperature. The excess presence of water prevented the inter-conversion of adsorbed species. These results suggest that addition of water to TEPA increases the adsorption capacity of the thin films by increasing the distance between TEPA molecules allowing adsorption of SO_2 through dative bonding. The presence of water also showed a decrease in SO_2-amine interactions allowing easy desorption of SO_2 from amines at temperatures as low as 70 ^{o}C. However, complete desorption of SO_2 from the films is not achieved.

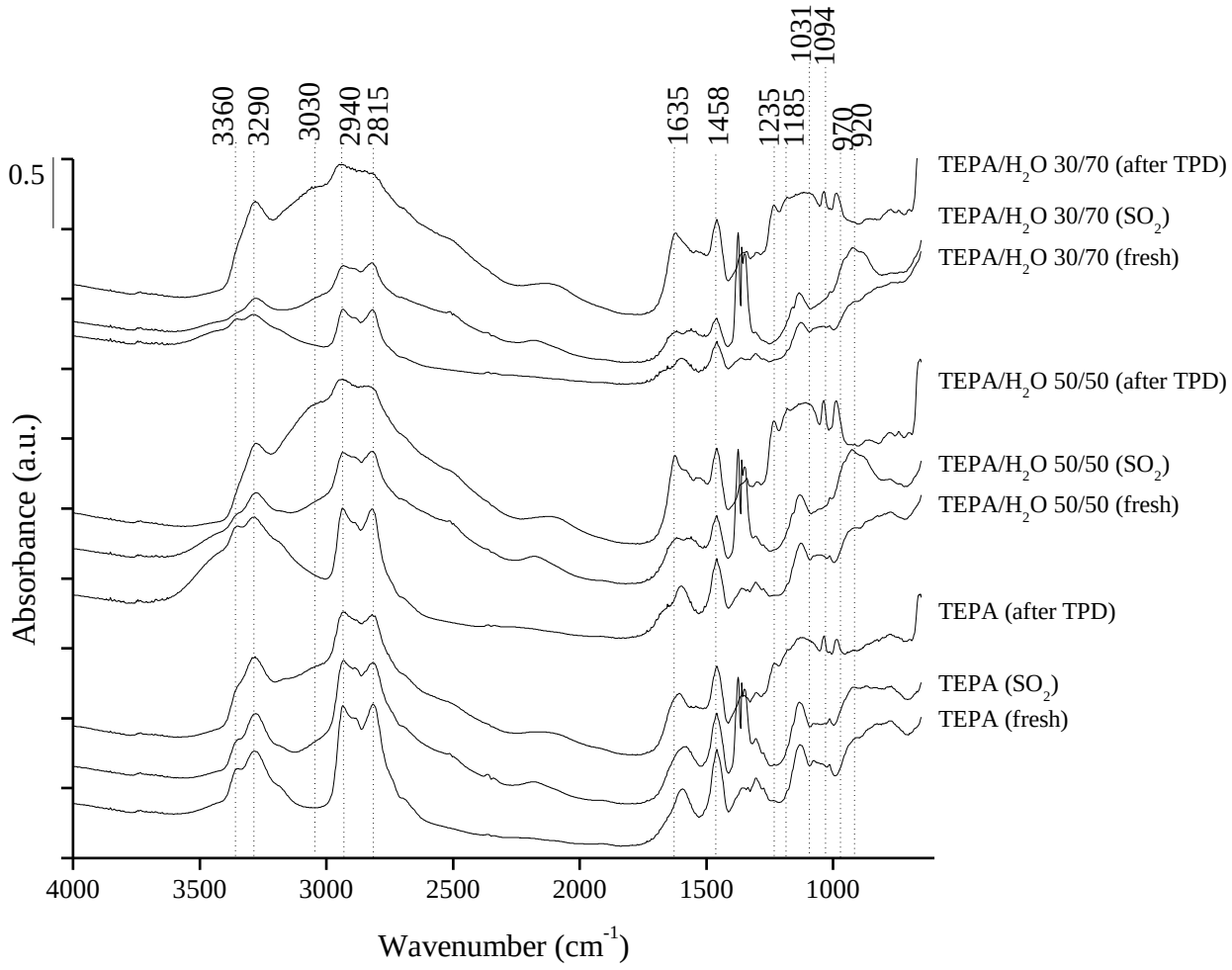

Figure 6 IR absorbance spectra of TEPA and TEPA/H_2O thin films after one cycle of SO_2 adsorption/desorption.

Figure 6 shows the IR absorbance spectra of TEPA and TEPA/H_2O thin films before SO_2 adsorption, during SO_2 adsorption, and after TPD. SO_2 adsorption on TEPA did not show a significant change in the intensity of amine stretching after SO_2 adsorption; indicating very poor adsorption of SO_2. Low adsorption of SO_2 on TEPA can be attributed to close packing of amine

sites and utilization of 4 amine sites for adsorption of SO_2 molecules i.e., $SO_2/N = 0.25$. This causes steric hindrance for adsorption of SO_2. On TEPA/H_2O samples, the conversion of double band at 3360 and 3290 cm^{-1} for asymmetric and symmetric stretching to a single peak centered at 3290 cm^{-1} is observed, and can be attributed to the increase in SO_2 adsorption capacity of the sample in the presence of water. The presence of water also produced strong bands at 920 and 970 cm^{-1} suggesting the increase in SO_2 adsorption on TEPA. The close-packing between TEPA molecules is minimized by the presence of water, which isolates the amine sites and allows SO_2 to adsorb through dative bonding using single amine site. The presence of water also reduces the steric hindrance caused by big units of sulfites and sulfates. The spectra after TPD showed the formation of bands between 1000-1300 cm^{-1} indicating the conversion of adsorbed species to bisulfate's and sulfates. The accumulation of species on TEPA/H_2O 50/50 is more compared to other samples. Increase in water content weakens the SO_2-amine interactions and allow for desorption at lower temperatures. Thus the presence of water not only improves the SO_2 adsorption capacity of amines but also decreases the temperature required for desorption.

Conclusions

SO_2 adsorption on TEPA and TEPA/H_2O thin film were studied in DRIFTS cell. Addition of water to TEPA minimized the packing between amine through hydrogen bonding formation between TEPA and water. SO_2 adsorption on TEPA produces ammonium ions, sulfites and sulfates as adsorbed species, with $SO_2/N = 0.25$. In the presence of water the adsorption capacity of the TEPA thin films was enhanced, where the SO_2 adsorption through dative bonding between nitrogen of amine to SO_2 where the $SO_2/N = 1$. The results indicate that in presence of water, the SO_2 adsorption capacity of the TEPA thin films enhanced. The presence of water not only enhances the adsorption capacity of TEPA thin films, but also decreases the temperature required for desorption of adsorbed species. Consequently water can be used as a solvent to enhance the SO_2 adsorption/desorption capacity of TEPA solutions.

4.4. Effect of PEG on SO_2 capture and SO_2 resistance of TPSENa sorbent

Table 4 shows SO_2 capture capacity of TPSENa, TPSENa-1P, TPSENa-5P and TPSENa-10P sorbents for 17 cycles. TPSENa degraded rapidly with 65% decrease in the initial capture capacity. TPSENa coated with PEG exhibits less degradation and the stability of the sorbent increases with the increase in the concentration of PEG in the coating. TPSENa-10 P has higher stability with only 40% decrease in the initial capture capacity than the other sorbents (60% decrease for TPSENa-1P and 55% decrease for TPSENa-5P) but with expense of low initial capture capacity (0.36 mmol/g-sorbent).

Table 4: SO_2 capture capacity and % decrease in the capture capacity after 17 cycles of TPSENa, TPSENa-1P, TPSENa-5P and TPSENa-10P sorbents

	Capture capacity (mmol/g-sorbent)			
cycle	TPSENa	TPSENa-1P	TPSENa-5P	TPSENa-10P
1	0.34	0.27	0.52	0.36
2	0.32	0.22	0.52	0.36
3	0.28	0.23	0.44	0.35
4	0.27	0.20	0.45	0.33
5	0.25	0.19	0.43	0.31
6	0.22	0.18	0.39	0.31
7	0.22	0.17	0.39	0.29
8	0.19	0.18	0.35	0.28
9	0.18	0.16	0.32	0.28
10	0.18	0.15	0.33	0.27
11	0.17	0.14	0.31	0.25
12	0.15	0.14	0.29	0.24
13	0.16	0.14	0.29	0.24
14	0.14	0.12	0.26	0.23
15	0.14	0.12	0.25	0.23
16	0.13	0.12	0.24	0.22
17	0.12	0.11	0.24	0.22
% decrease	64.71	59.25	53.85	38.89

Figure 20 shows normalized SO_2 MS profile during (i) pretreatment, (ii) SO_2 adsorption, (iii) Ar purge and (iv) after TPD of one SO_2 capture cycle over TPSENa. MS Intensity rises as soon as the inlet gas is switched from Ar to SO_2 via 4-port valve and reaches to its maximum. Once

the equilibrium is attained, SO_2 MS intensity remains at the maximum. SO_2 MS profile drops to the baseline when the inlet gas is switched back to Ar for purging. Weakly adsorbed SO_2 are purged out during Ar purge. SO_2 MS profile rises again when the temperature of the sorbent is increased during TPD, indicating that the SO_2 is being desorbed form the sorbent. The changes in the surface characteristics of the sorbent can be determined by the single beam and absorbance spectra taken during (i) pretreatment, (ii) SO_2 adsorption, (iii) Ar purge and (iv) after TPD.

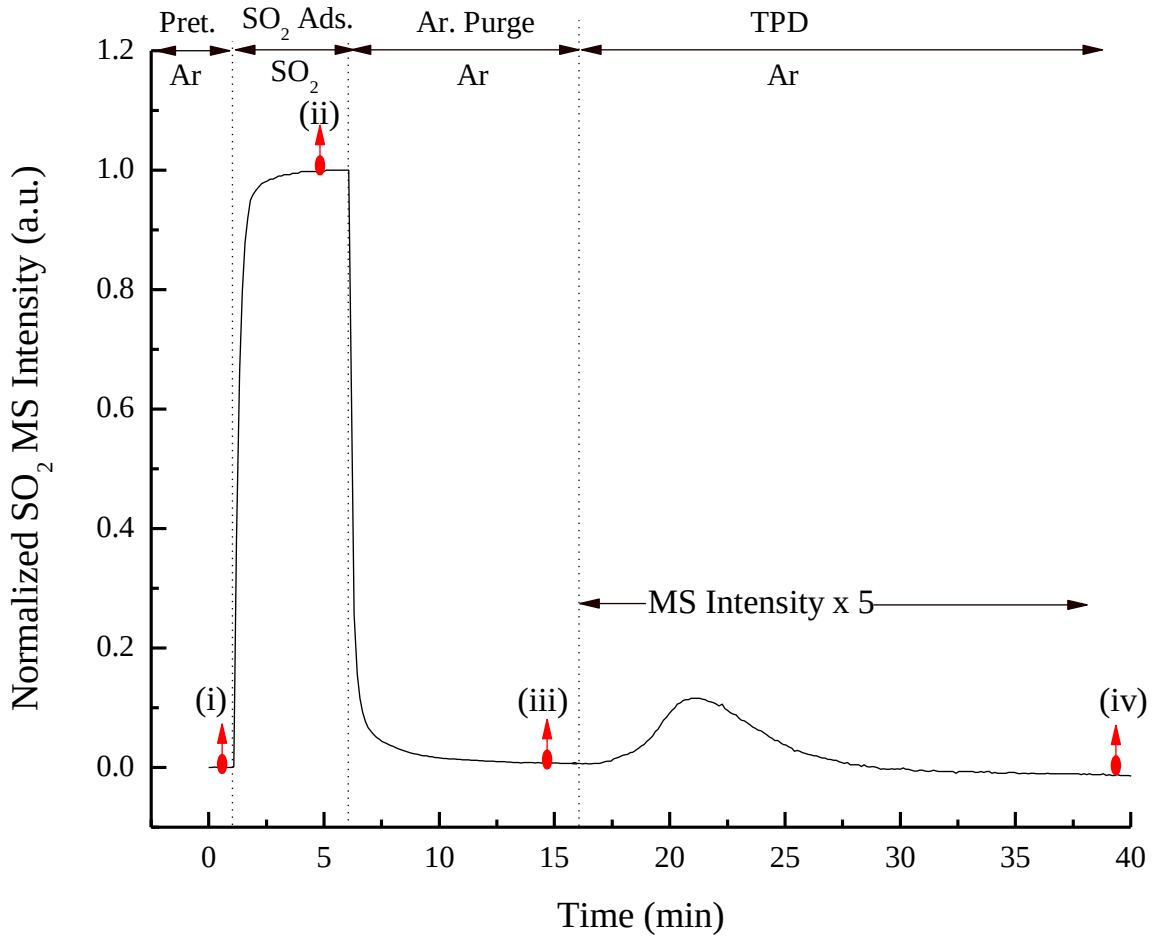

Figure 20: Normalized SO_2 MS profile(m/e=64) during (i) pretreatment. (ii) SO_2 adsorption, (iii) Ar purge and (iv) after TPD of SO_2 capture cycle.

Figure 21(a) shows the single beam spectrum taken each step shown in Figure 20. The changes on the surface of the sorbent during these steps are discerned in the absorbance spectra. Figure 21(b) shows the absorbance spectra taken during pretreatment, SO_2 adsorption, Ar purge and after TPD. Absorbance spectra are obtained using single beam spectrum during pretreatment as background. Peaks at 1377 and 1342 cm^{-1} in the absorbance spectrum during SO_2 adsorption indicate the gas phase SO_2. Formation of the peaks at 1690, 1650, 1462 (sulfite) and 1011 cm^{-1}

(bi sulfate) indicate the formation of SO_2 adsorbed species. Broad absorption peaks at 2623 and 2457 cm^{-1} are similar to the zwitterions formed during CO_2 adsorption over solid amine sorbent, suggesting that the SO_2 adsorption over solid amine sorbent may produce zwitterions as intermediate species like that of CO_2. Absorption peak at 3005 cm^{-1} indicates the formation of ammonium ion during SO_2 adsorption. The peak centering at 3461 cm^{-1} is caused due to the interaction between hydroxyl hydrogen atoms of PEG and SO_2[10,23]. The absorbance spectrum during Ar purge has similar features as spectrum during adsorption. The intensity of the peaks decreased as some of the weakly adsorbed SO_2 species were purged during Ar purge.

Height of the absorbance peaks of SO_2 adsorbed species (1011, 1689 cm^{-1}), Zwitterion (2457, 2622 cm^{-1}), Ammonium ion (3005 cm^{-1}) and 3462 cm^{-1} were determined for TPSENa, TPSENa-1P, TPSENa-5P, TPSENa-10P sorbents. For a qualitative comparison among different sorbents, the ratio of intensity of the peaks at 1011, 1689, 2457, 2622, 3005, 3462 cm^{-1} to intensity of 3462 cm^{-1} for different sorbents are compared. Increase in the ratio implies that the formation of that specific species is increased.

Figure 22(a) shows the ratio of intensity of peaks at 1011, 1689, 2457, 2622, 3005, 3462 cm^{-1} to intensity of 3462 cm^{-1} for TPSENa-1P, TPSENa, TPSENa-10P and TPSENa-5P sorbents for cycle 1. The sorbents were rearranged with increasing capture capacity. The ratio of peak intensity of SO_2 adsorbed species (1011, 1689 cm^{-1}) to intensity of the peak at 3462 cm^{-1} increase for the sorbent with higher capacity and vice versa. TPSENa-5P is expected to have a higher peak ratio for 1011 cm^{-1} (bisulfate), but it was off the trend.

The capture capacity of the sorbent is also proportional to the formation of zwitterions (2622 and 2457 cm^{-1}). TPSENa-5P which has high initial capture capacity has higher ratio when compared to other sorbents. Formation of ammonium ion during SO_2 adsorption is more in TPSENa sorbent, because of the closely packed amine sites present in the sorbent. PEG disperses the amine sites present in sorbent and therefore the formation of ammonium ions becomes more difficult. Increase in the concentration of PEG in the coating decreases the formation of ammonium ion.

The peak ratio of 3005 cm^{-1} (ammonium ion) is expected to decrease as the concentration of PEG in the coating increases. The peak ratio decreased drastically for TPSENa-1P sorbent, but the ratio increased again with further increase in the concentration of PEG in the coating suggesting that the surface coating of PEG has different chemistry than addition of PEG in the bulk. Figure 22(b) shows the ratio of intensity of peaks at 1011, 1689, 2457, 2622, 3005, 3462 cm^{-1} to intensity of 3462 cm^{-1} for TPSENa-1P, TPSENa, TPSENa-10P and TPSENa-5P sorbents for cycle 17. It shows similar trend as in Figure 22(a) indicating that, exposing the sorbent to SO_2 to 17 cycles did not alter the adsorption mechanism or composition of the sorbent.

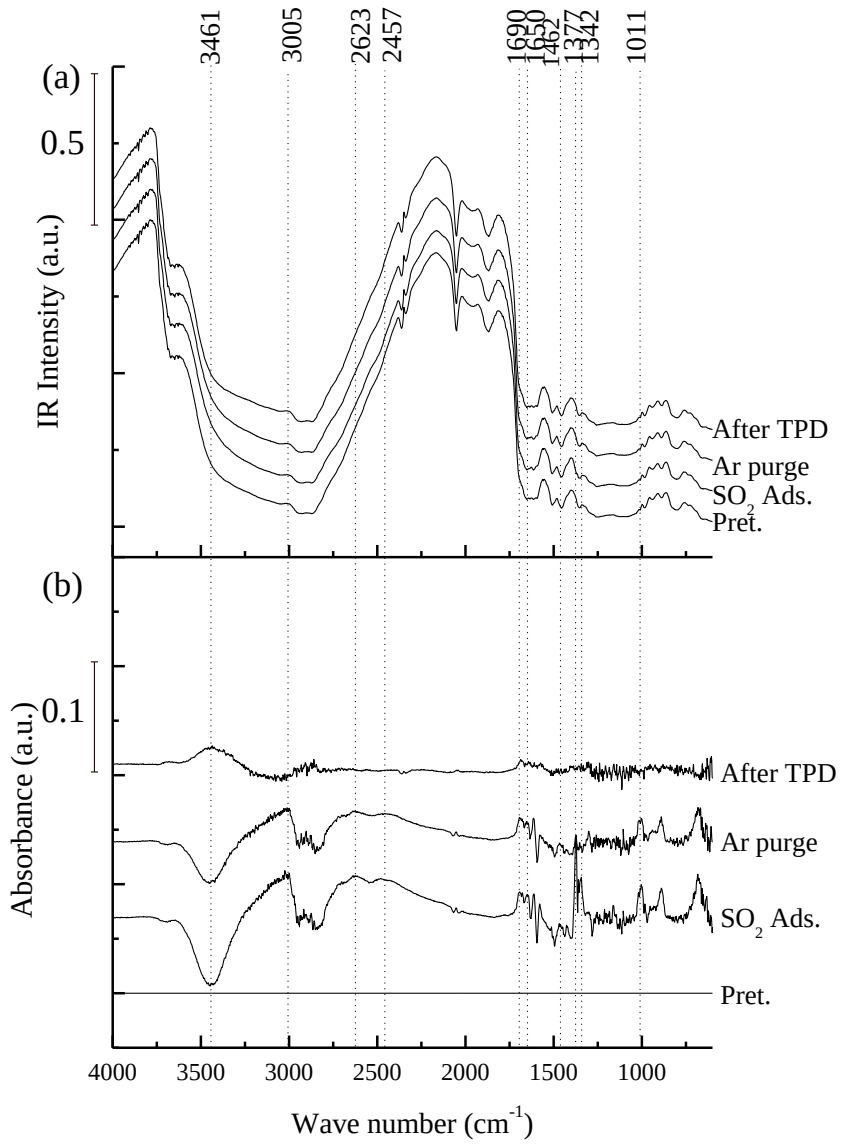

Figure 21: (a) Single beam spectra taken during pretreatment, SO_2 adsorption, Ar purge and after TPD (b) absorbance spectra during pretreatment, SO_2 adsorption, Ar purge and after TPD. Absorbance=log(I_o/I) where, I_o is single beam spectrum taken during pretreatment and I, is the single beam spectra taken during pretreatment, SO_2 adsorption, Ar purge and after TPD.

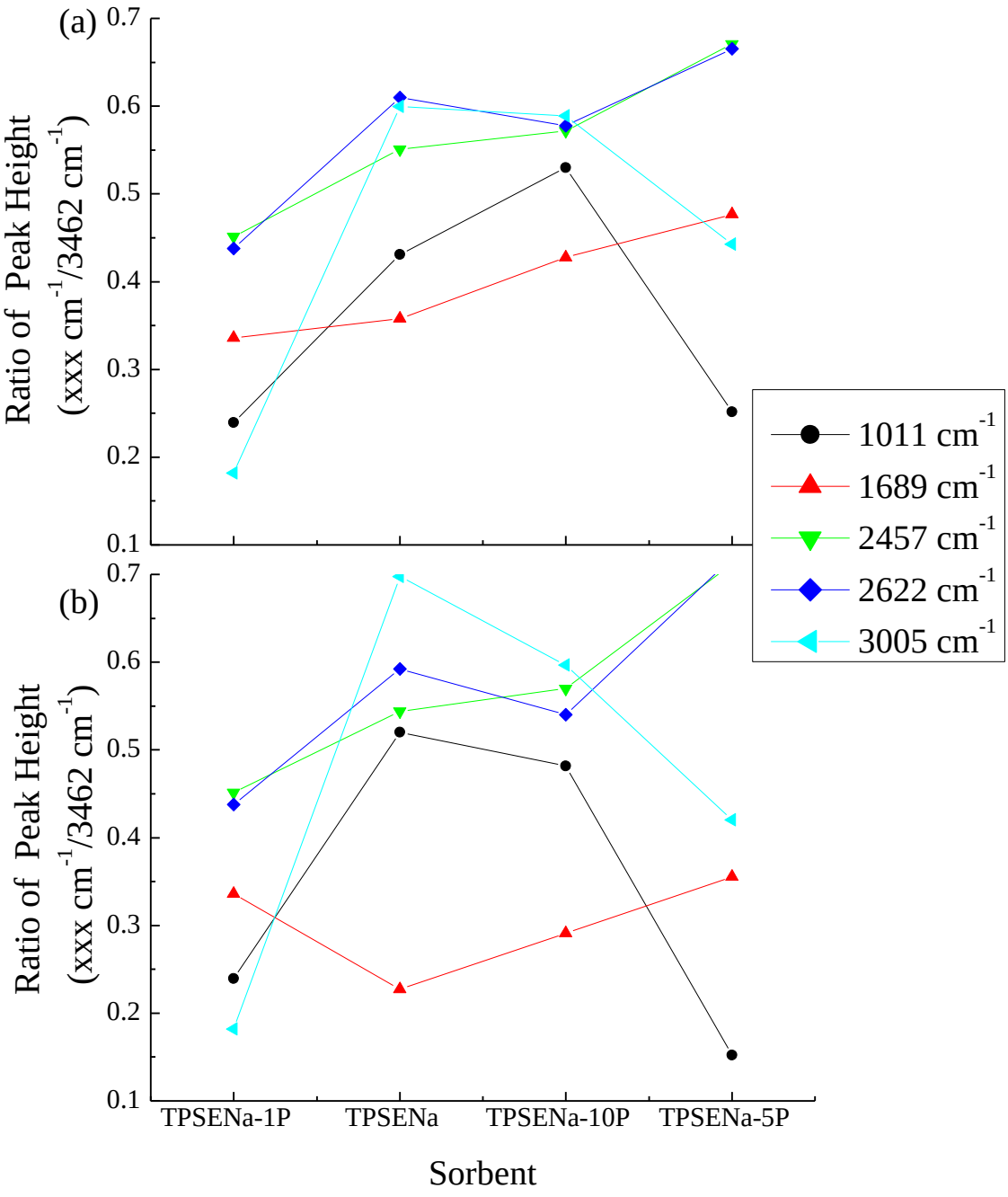

Figure 22: (a) Comparison of the maximum intensity of the absorbance peaks at 1011, 1689, 2457, 2622, 3005, 3462 cm^{-1} for TPSENa, TPSENa-1P, TPSENa-5P, TPSENa-10P-cycle 1 and (b) Comparison of the maximum intensity of the absorbance peaks at 1011, 1689, 2457, 2622, 3005, 3462 cm^{-1} for TPSENa, TPSENa-1P, TPSENa-5P, TPSENa-10P-cycle 17

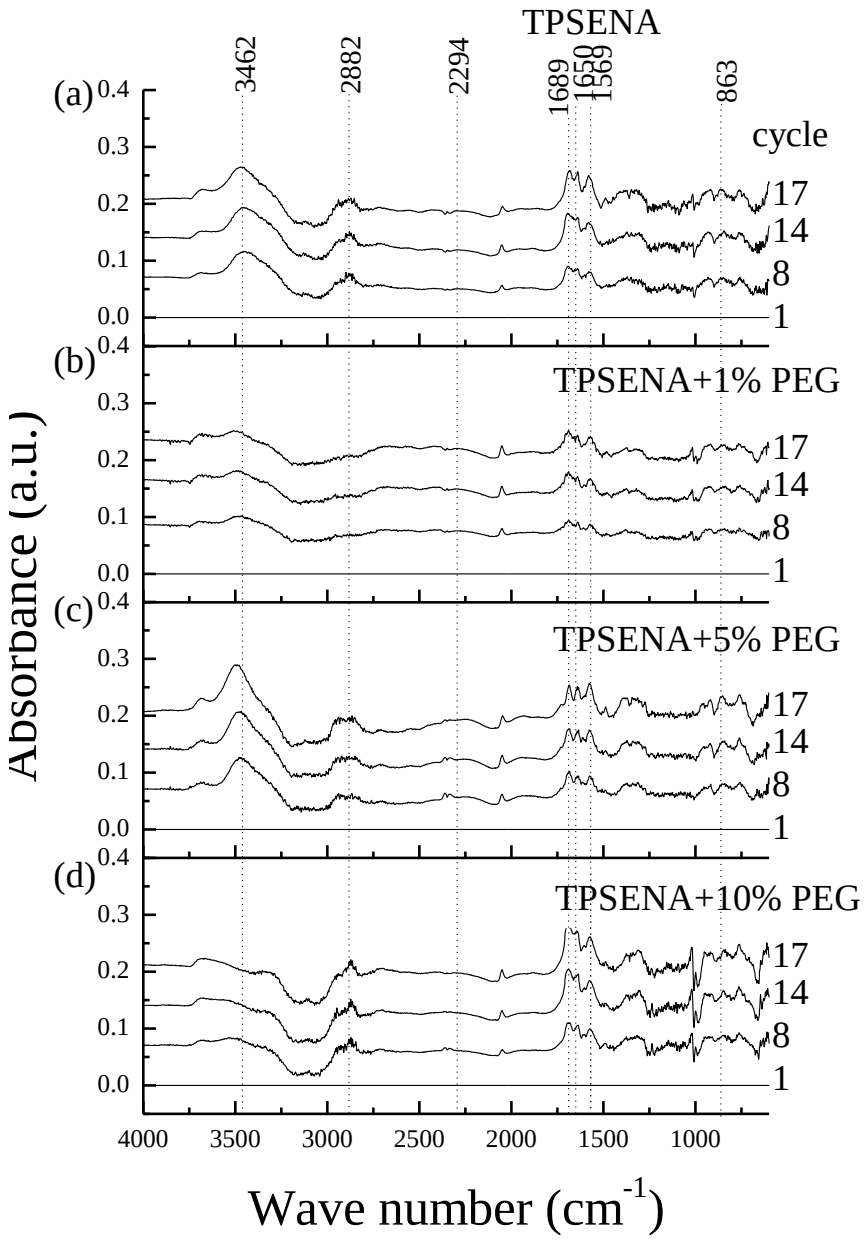

Figure 23: Absorbance spectra after TPD of 1, 8, 14 and 17 cycles for (a) TPSENa, (b) TPSENa-1P, (c) TPSENa-5P and (d) TPSENa-10P sorbent. Absorbance=log(I_o/I) where, I_o is single beam spectrum taken after TPD of cycle 1 and I, is the single beam spectra taken after TPD of cycle 1, 8, 14 and 17.

Figure 23 shows the absorbance spectra taken after TPD of cycles 1, 8, 14 and 17 of (a) TPSENa, (b) TPSENa-1P, (c) TPSENa-5P and (d) TPSENa-10P sorbents. Single beam spectrum taken after TPD of cycle 1 is taken as background to obtain the absorbance spectra. Presence of absorbance peaks at 1689, 1650 and 1569 cm^{-1} (bisulfate) indicate the accumulation of SO_2 adsorbed species. Accumulation of species indicates that the sorbent is not completely regenerated after TPD. For the sorbents with higher concentration of PEG in the coating

(TPSENa-5P, TPSENa-10P), there is less decrease in the capture capacity even in the presence of accumulated species. Thus increasing the concentration of PEG in the coating increases the stability of the sorbent, but in expense of the initial capture capacity.

Conclusions

TPSENa degraded rapidly with 65% decrease in the initial capture capacity. TPSENa coated with PEG exhibits less degradation and the stability of the sorbent increases with the increase in the concentration of PEG in the coating. TPSENa-10 P has higher stability with only 40% decrease in the initial capture capacity than the other sorbents (60% decrease for TPSENa-1P and 55% decrease for TPSENa-5P) but with expense of low initial capture capacity (0.36 mmol/g-sorbent).

4.5. Effect of SO_2 on CO_2 capture of TPSENa sorbent

Figure 24(a) andFigure 24(b) show MS profile of SO_2 during 30 cycles of CO_2 capture over TPSENa-P sorbent in presence of 40 ppm and 100 ppm SO_2. Rise in the SO_2 MS intensity during CO_2 adsorption indicates the presence of SO_2 in the inlet gas stream and also confirms that the mass spectrometer is capable to detect the presence of SO_2 at 40 ppm. The MS intensity of SO_2 rises to 9E-14 in presence of 40 ppm SO_2 and to 2E-13 in presence of 100 ppm SO_2 which is twice the intensity in presence of 40 ppm.

Figure 25(a) and Figure 25(b) show CO_2 MS profile during 30 cycles of CO_2 capture over TPSENa-P in presence of 40 ppm and 100 ppm SO_2. Decrease in the CO_2 MS intensity during TPD after 5^{th} cycle suggests the decrease in the performance of the sorbent. In presence of 100 ppm SO_2, the CO_2 MS profile decreased more rapidly during TPD when compared to 40 ppm SO_2. Table 5 shows the CO_2 capture capacity of the sorbent in presence of 40 and 100 ppm of SO_2 in inlet gas stream. The decrease in capture capacity of the sorbent was 50% in presence of 40 ppm SO_2 and by 60% in presence of 100 ppm SO_2. Presence of SO_2 even at low concentration such as 40 ppm causes the sorbent to degrade and increase in the concentration of SO_2 in the inlet gas stream aggravates the degradation.

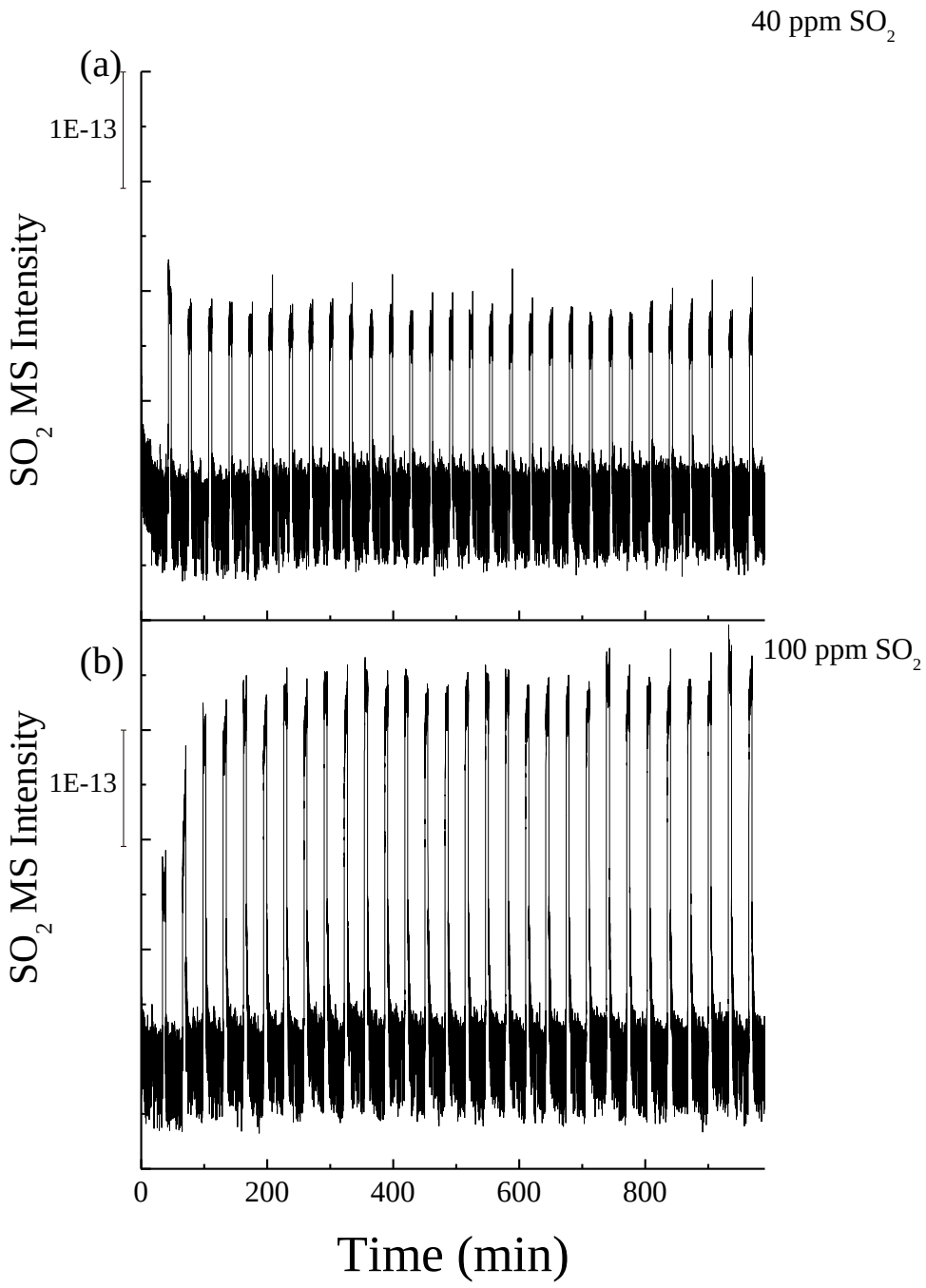

Figure 24: SO_2 MS profile during 30 cycles of CO_2 capture over TPSENa-P in presence of (a) 40 ppm SO_2 and (b) 100 ppm of SO_2

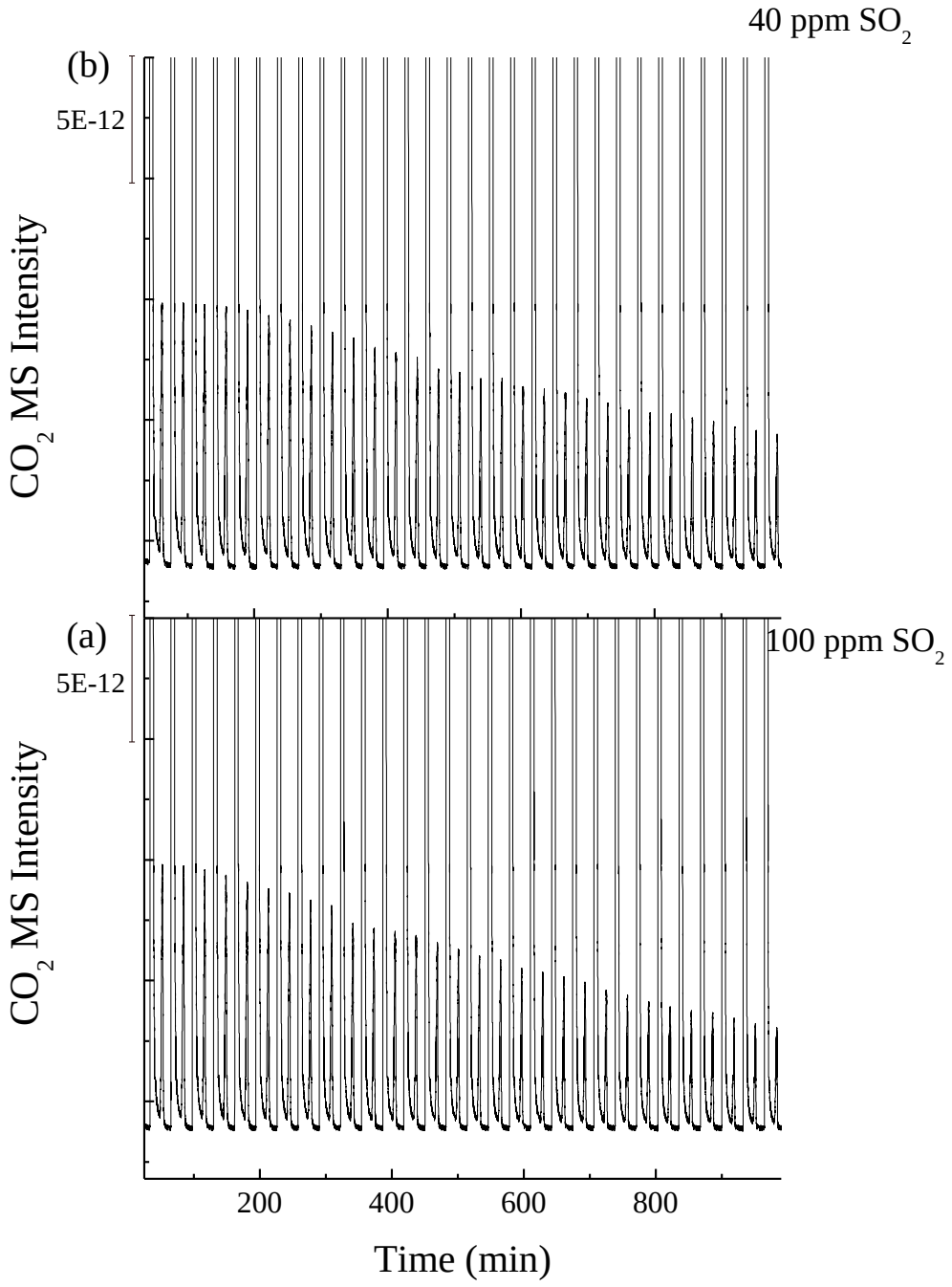

Figure 25: CO_2 MS profile during 30 cycles of CO_2 capture over TPSENa-P in presence of (a) 40 ppm SO_2 and (b) 100 ppm of SO_2

Figure 26(a) and Figure 26(b) show the IR-absorbance spectra during Ar purge of 1, 2, 5, 10, 15, 20, 25 and 30 cycles of CO_2 capture in presence of 40 and 100 ppm SO_2. Absorbance spectra are obtained by taking single beam spectrum prior to CO_2 adsorption as background. Absorption peak centered at 3005 cm^{-1} suggests the formation NH_3^+ species. Absorption peaks at1633 cm^{-1} (C=O), 1564 and 1412 cm^{-1} (C-N) suggests the formation of carbamates. Decrease in the intensities of the absorption peaks at 3000, 1633, 1564 and 1412 cm^{-1} with the number of adsorption and desorption cycles performed suggests the decrease in the formation of carbamate species during CO_2 adsorption. The decrease in the formation of carbamates is due to the accumulation of the bisulfate species formed due to presence of SO_2 in the inlet gas stream. The absorbance spectrum in Figure 26(b) exhibits similar absorption features as in figure 26(a). Formation of bisulfates (1010 and 889 cm^{-1}) can be seen more clearly in presence of higher SO_2 concentration. The absorption intensities decreased more rapidly in presence of higher SO_2 concentration due to the accumulation of more sulfate species resulting in rapid degradation of the sorbent.

Table 5: CO_2 capture capacity of TPSENa-P in presence of 40 and 100 ppm SO_2

cycle	mmol-CO_2/g-sorbent	
	40 ppm	100 ppm
1	1.05	1.12
2	1.01	1.12
5	0.95	1.04
10	0.84	0.90
15	0.76	0.82
20	0.68	0.66
25	0.61	0.55
30	0.55	0.45
%decrease in capture capacity	47.69	59.64

Figure 27 shows the absorbance spectra taken after TPD of cycles 1, 2, 5, 10, 15, 20, 25 and 30 for CO_2 capture in presence of (a) 40 and (b) 100 ppm SO_2. Absorbance spectra are obtained by taking single beam spectrum after TPD of first cycle as the background. Increase in the accumulation of CO_2 adsorbed species and bisulfates, with the increase in the SO_2 concentration can be verified by the increase in the intensities of absorption peaks in Figure 27(a) andFigure

27(b). Increase in the absorption peaks at 3005cm^{-1} shows the accumulation of ammonium ion. Formation of absorption peaks at 2559, 1633, 1534 and 1412 cm^{-1} with the repetitive adsorption and desorption cycles indicates the accumulation of CO_2 adsorbed species. Growth of peaks at 986 and 803 cm^{-1} indicates the accumulation of bisulfates on the surface of the sorbent. Decrease in absorption intensities at 3362 and 3302 cm^{-1} suggests the deactivation of amine sites due to the accumulated species.

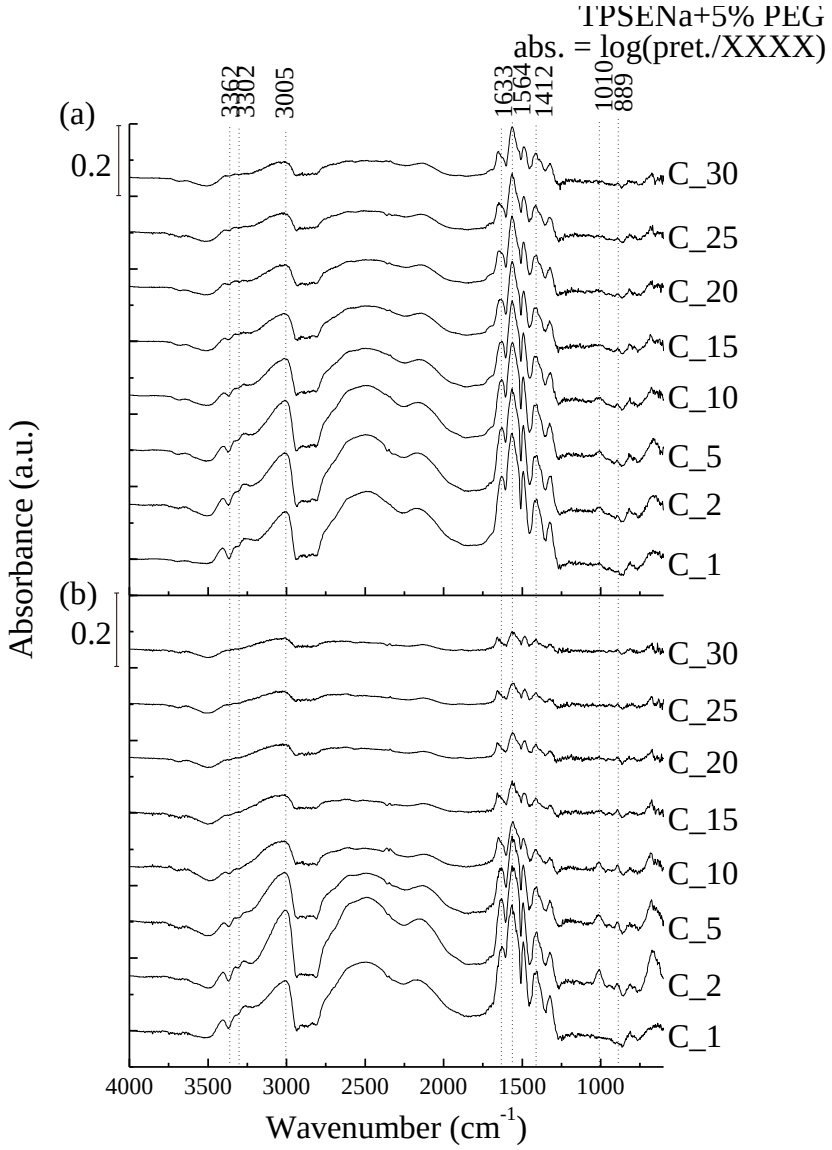

Figure 26: Absorbance spectra prior TPD for cycles 1, 2, 5, 10, 15, 20, 25 and 30 over TPSENa-P in presence of (a) 40 ppm (b) 100 ppm SO_2. Absorbance=log (I_o/I), where, I_o is single beam taken during pretreatment of each cycle and I is corresponding single beam taken before TPD of the corresponding cycle.

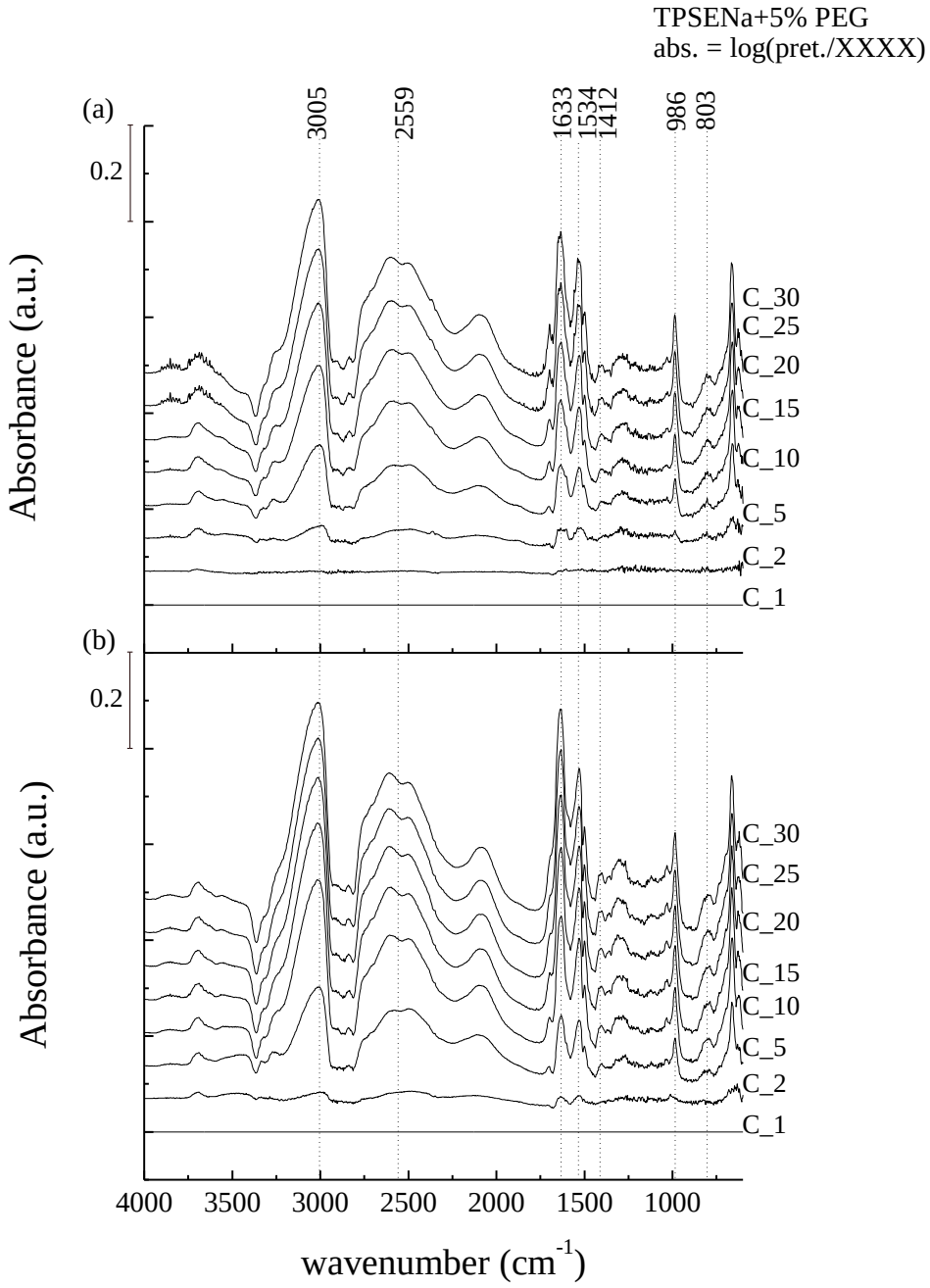

Figure 27: Absorbance spectra after TPD for cycles 1, 2, 5, 10, 15, 20, 25 and 30 in presence of (a) 40 ppm of SO_2 and (b) 100 ppm SO_2. Absorbance=log (I_o/I), where, I_o is single beam taken after TPD of first cycle and I is corresponding single beam taken during adsorption of each cycle.

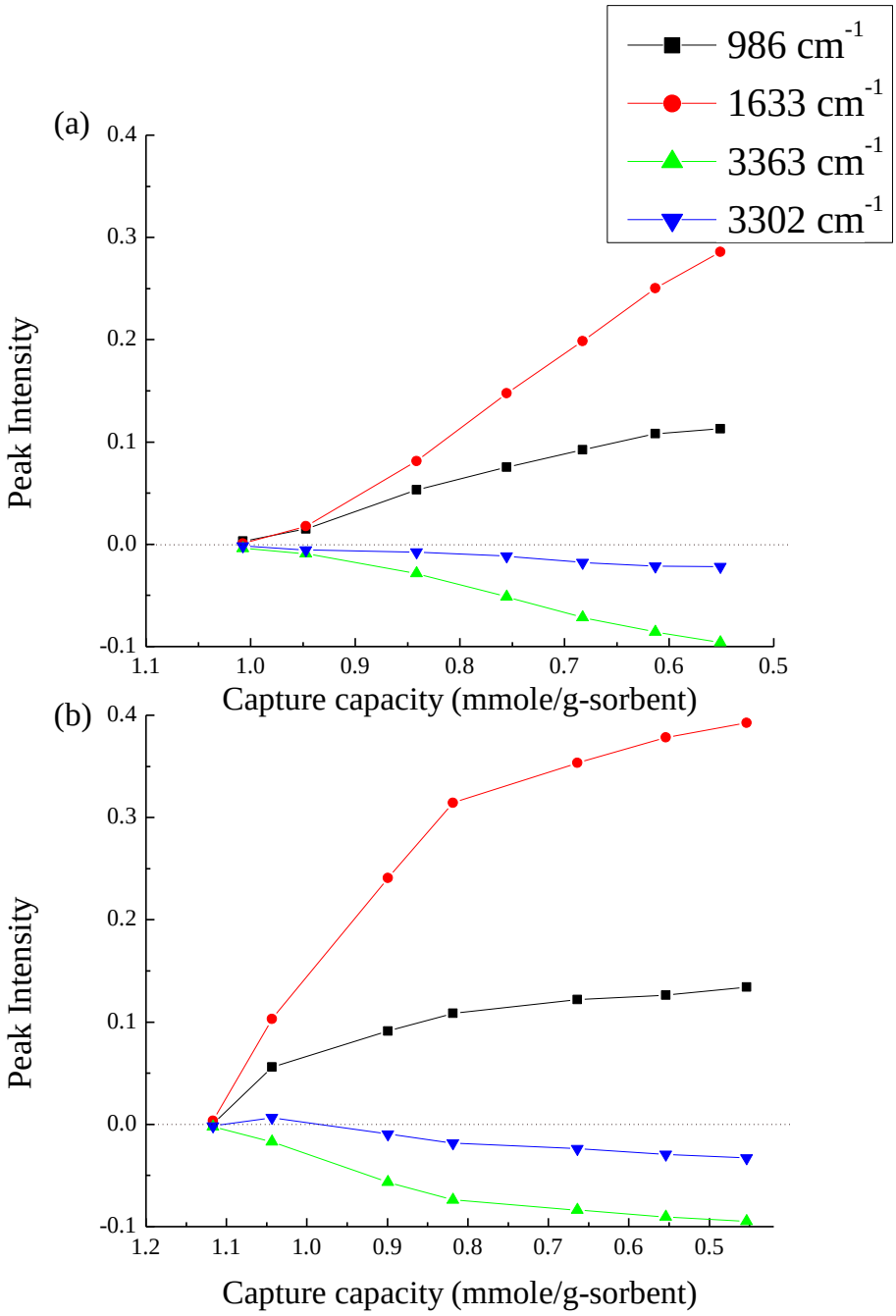

Figure 28: Peak heights of 986 cm^{-1}, 1633 cm^{-1}, 3363 cm^{-1}, 3302 cm^{-1} with respect to capture capacity for (a) CO_2 capture in presence of 40 ppm SO_2 and (b) CO_2 capture in presence of 100 ppm SO_2

Figure 28(a) and Figure 28(b) shows the intensity of absorption peaks at 3363, 3302, 1633 and 986 cm^{-1} from figure 27(a) and 27(b) Vs the capture capacity of the sorbent. Capture capacity of the sorbent is inversely proportional to the accumulation of carbamates and bisulfates on the surface of the sorbent. Accumulation of carbamates and bisulfates are evidenced by the increase in the intensity of peaks at 1633 and 986 cm^{-1}. Deactivation of amine sites are evidenced by the decrease in absorption intensities at 3362 and 3302 cm^{-1}. As the concentration of SO_2 increases, the accumulation of the carbamates and bisulfates increased which results in lower capture capacity of the sorbent.

Conclusions

Presence SO_2 in the inlet gas stream at low concentration such as 40 ppm leads to degradation of the sorbent due to the accumulation of SO_2 adsorbed species on the surface of the sorbent. Higher concentration of the SO_2 in the inlet gas stream aggravates the degradation of sorbent.

4.6. Effect of SO_2 and H_2O on CO_2 capture of TPSENa sorbent

Figure 29 shows MS intensity profile of a gas species during a typical CO_2 capture cycle. The MS profile rises as soon as the inlet gas is switched from Ar to simulated flue gas and reaches to its maximum. The MS intensity drops to its baseline when the inlet gas stream is switched from simulated flue gas to Ar. The MS intensity of a gas is calculated from the difference between the maximum intensity and its baseline.

SO_2250C^{wet} is a unique case, illustrated in Figure 30., which will be discussed first. Figure 30 shows the H_2O, N_2, O_2, Ar, CO_2, and SO_2 MS profiles during CO_2 capture cycles in presence of 250 ppm SO_2/4% H_2O where, SO_2 was flowing continuously throughout CO_2 capture cycles (path c in figure 1). SO_2 MS intensity did not rise until 200^{th} min because of the poor mixing of gas streams due to large difference in the flow rates (Table 1). Drop in the the max. MS intensity of Ar, CO_2, N_2, and O_2 suggests a leak in the system. Figure 30 shows that the CO_2 gas phase intensity was 30% less during 30^{th} cycle when compared to the 1^{st} cycle indicating a leak in the system.

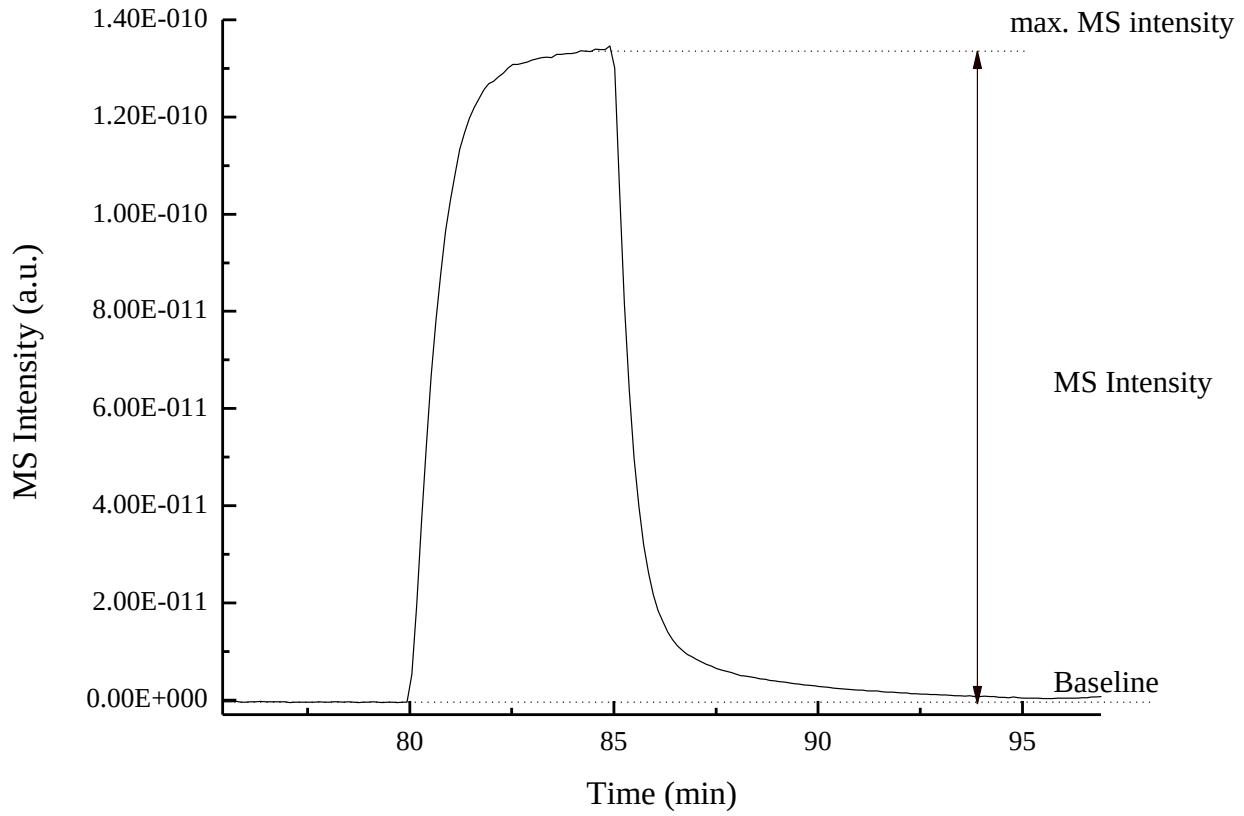

Figure 29: MS intensity profile of a gas species during a typical CO_2 capture cycle.

Figure 30 shows H_2O, N_2, O_2, Ar, CO_2, and SO_2 MS profiles during CO_2 capture cycles in presence of 250 ppm SO_2/4% H_2O where, SO_2 was flowing during CO_2 adsorption step (path B in figure 1). The SO_2 MS intensity rose only for 10 sec during 1st cycle and dropped to the baseline. The substantial drop in MS intensity indicates a flow imbalance caused by the pressure drop generated by the solenoid valve. The imbalance in SO_2 flow causes the deviation of SO_2 concentration from the set point.

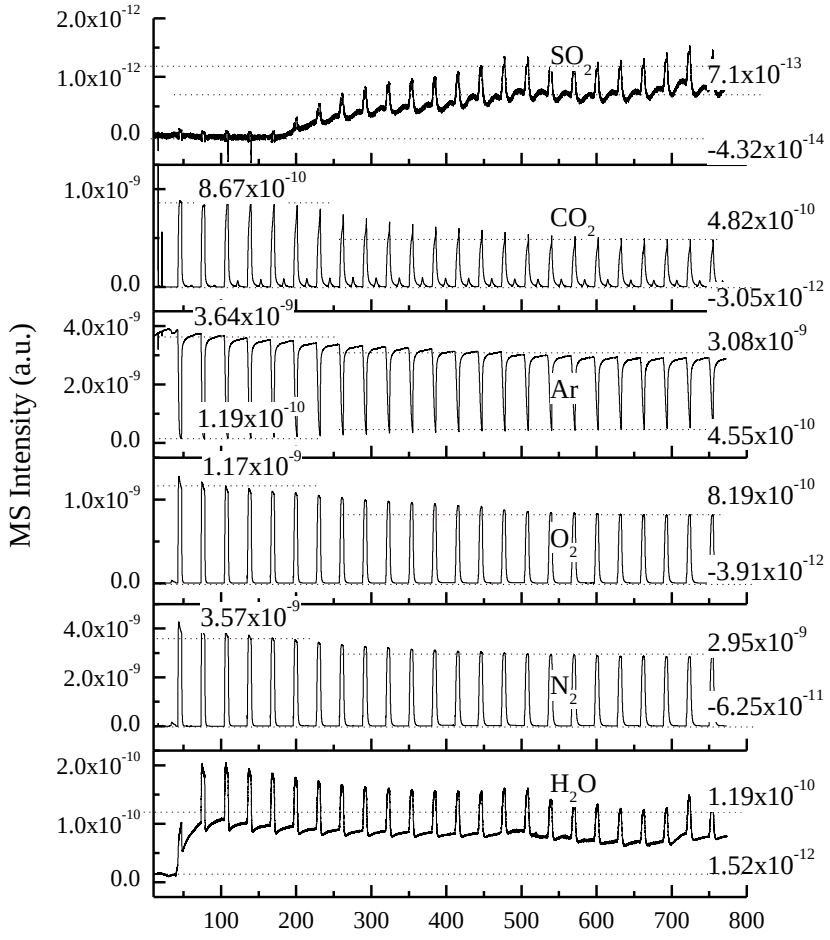

Figure 30: H_2O, N_2, O_2, Ar, CO_2 and SO_2 MS profiles during CO_2 capture study in presence of 250 ppm SO_2 and water (SO_2250C^{wet}).

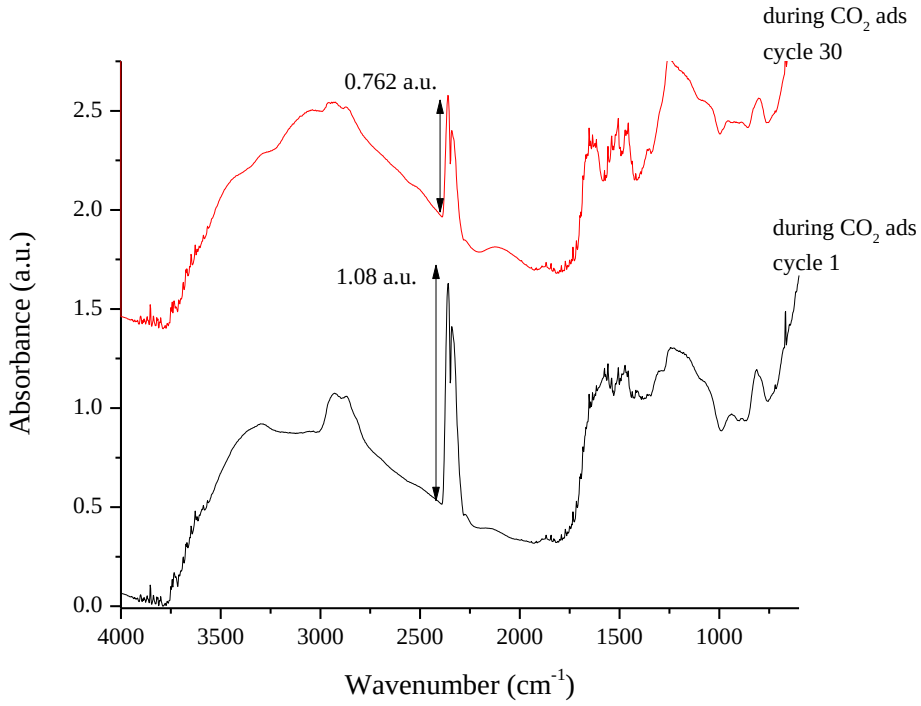

Figure 31: Comparison of absorbance spectra during CO_2 adsorption of cycle 1 and 30 (SO_2250C^{wet}).

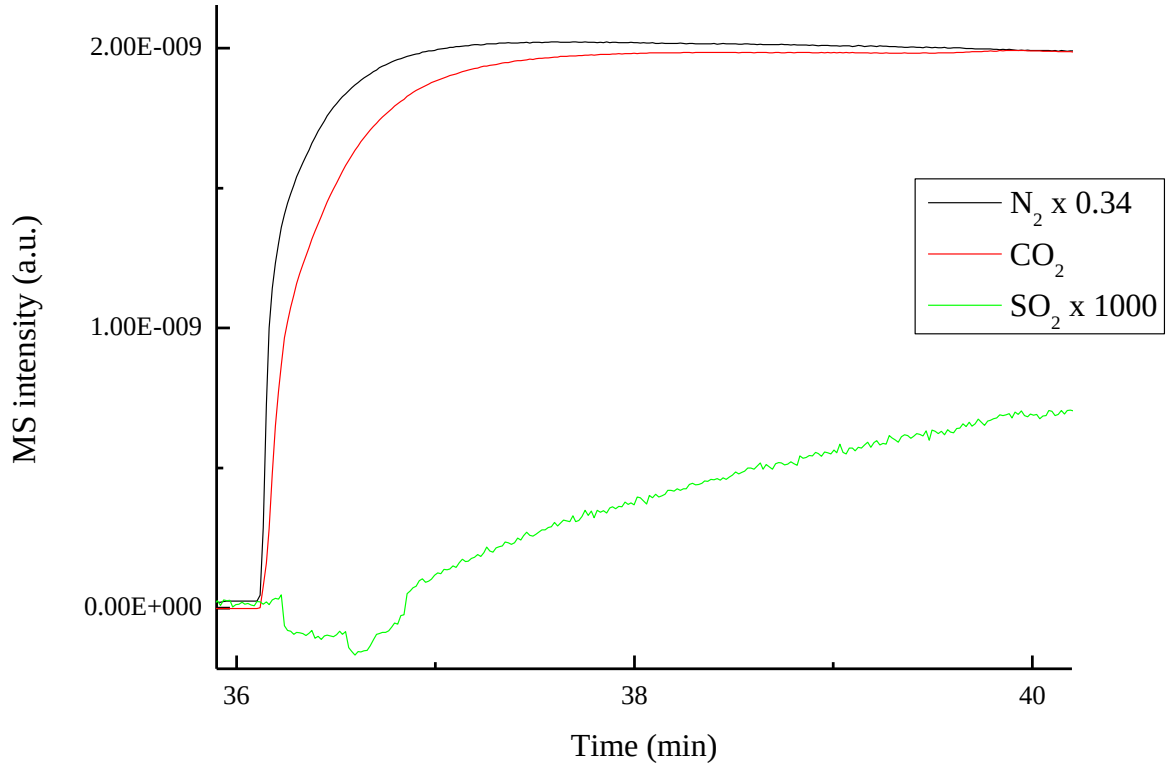

Figure 32: N_2, CO_2, and SO_2 break through curve during a typical CO_2 capture cycle ($SO_2$40A^{dry})

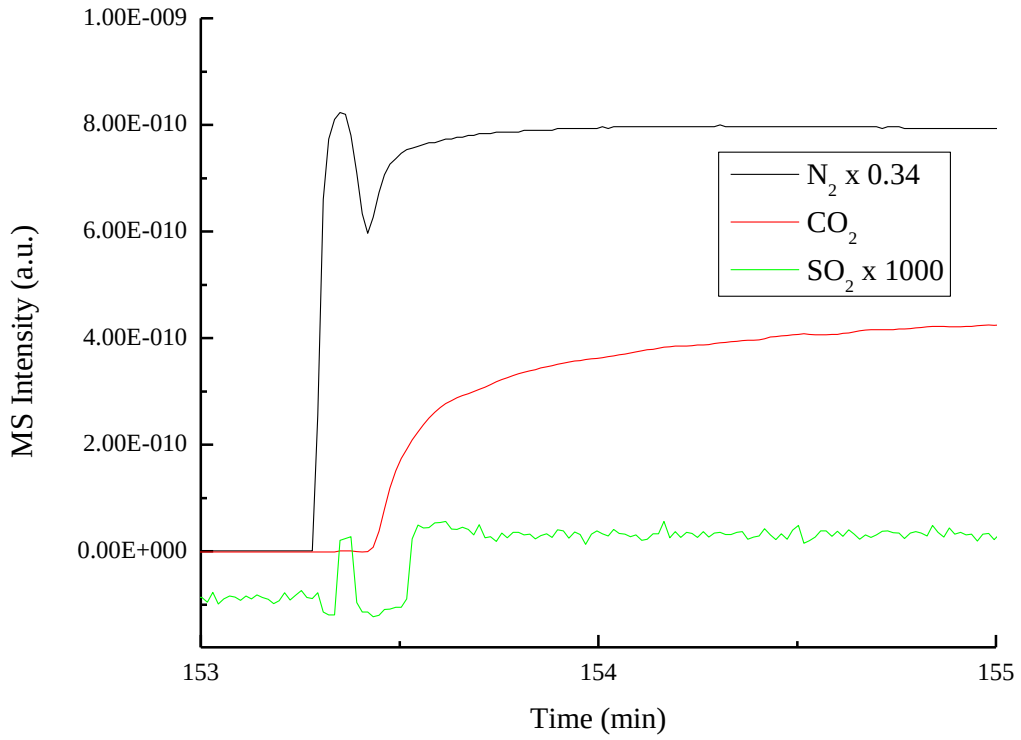

Figure 33: N_2, CO_2, and SO_2 break through curve during a typical CO_2 capture cycle ($SO_2$40B^{dry})

Figure 34 **Error! Reference source not found.** show the lag in SO_2 MS intensity during CO_2 adsorption step indicating the sluggish SO_2 mixing in the inlet gas stream. Table 6 shows the CO_2 capture capacity of amine sorbent in presence SO_2 in dry and wet conditions. The amine sorbent degraded less in wet conditions (22.26% for $SO_2$40B^{wet} and 22.14% for $SO_2$250B^{wet}) when compared to CO_2 capture cycles performed in dry conditions (44.26% for $SO_2$40A^{dry} and 32.35% $SO_2$40B^{dry}). The sorbent exhibited same %degradation at both 40 and 250ppm SO_2 which suggests that there are flow disturbances in the system. The CO_2 capture capacity increased during CO_2 capture cycles in presence of 250 ppm SO_2/4% H_2O, where SO_2 was flowing continuously throughout CO_2 capture cycles The ratio of sulfur to silica in the sorbent after the CO_2 capture cycles is determined by the XRF. The sorbent exposed to 250 ppm SO_2/4% H_2O exhibited less amount of sulfur deposition when compared to the sorbent exposed to 40 ppm SO_2 both in dry and wet conditions. The IR absorbance spectra also showed less accumulation of species in presence of 250 ppm SO_2 when compared to 40 ppm SO_2 which indicates the deviation of SO_2 concentration from the set point.

Table 6: CO_2 capture capacity of the amine sorbent during CO_2 capture in presence of SO_2/H_2O and SO_2

Experiment	CO_2 Capture Capacity ($mmol_{CO2}/g_{sorb}$)					% Decrease	S/Si Ratio (mol%)
	Cycle 1	Cycle 2	Cycle 10	Cycle 20	Cycle 25		
$SO_2$40A^{dry}	0.98	0.91	0.70	0.59	0.54	44.26	0.97
$SO_2$40B^{dry}	1.25	1.21	1.11	0.95	0.90	32.35	0.19
$SO_2$40B^{wet}	1.30	1.27	1.22	1.07	1.01	22.26	0.18
$SO_2$250B^{wet}	1.45	1.28	1.20	1.10	1.13	22.14	-
$SO_2$250C^{wet}	1.30	8.11	6.31	5.89	1.30	-	0.03

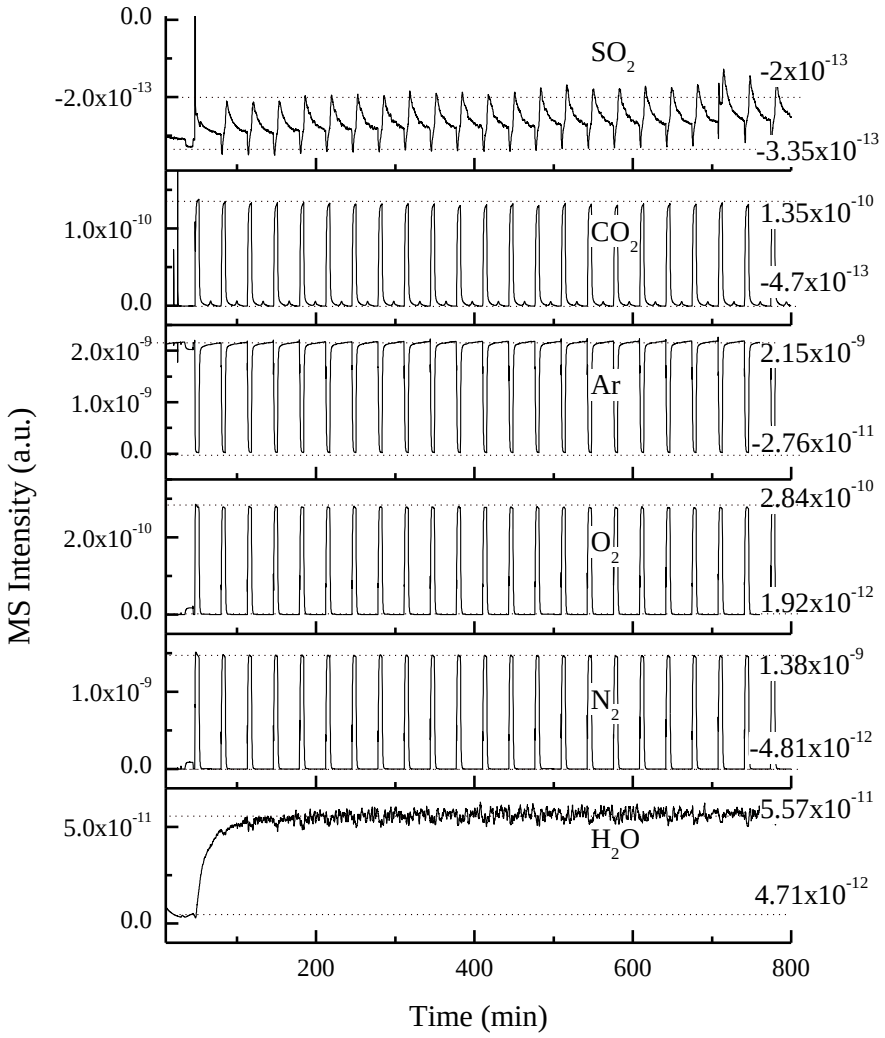

Figure 34: H_2O, N_2, O_2, Ar, CO_2 and SO_2 MS profiles during CO_2 capture study in presence of 250 ppm SO_2 and water (SO_2250B^{wet}).

Conclusions:

- The deviation of SO_2 concentration from the set point leads to over/under estimation of the sorbent capture capacity and stability.
- Improper control of the SO_2 concentration in the inlet gas stream is due to the flow imbalances caused by poor mixing of gas streams. Proper mixing of gas streams can be achieved by, (i) avoiding large difference in the flow rates of the gas streams, (ii) using 'wye' instead of 'tee' connecters to mix the gas streams. Wye connects enhances the gas mixing even if gas streams of different flow rates are used, and (iii) using the check valves to avoid the back pressure in the gas streams.
- The mass spectrometer has to be calibrated prior to the experiment to estimate the concentration of SO_2 in the inlet gas mixture accurately. The calibration is performed by

injecting the known concentrations of SO_2 to the mass spectrometer. The inlet of the mass spectrometer is connected to the carrier gas flowing at a same flow rate as the carrier gas in the CO_2 capture cycles. An empty tube with a volume equal to the volume of DRIFTs is connected in between the injection port and the mass spectrometer. The empty tube act as dead volume. Both Ar and CO_2/air will be tested as carrier gas to study the effect of carrier gas on the calibration of mass spectrometer.

- The mass ratio of N_2/O_2 in air is 3.26 and the calculated N_2(m/e=28)/O_2(m/e=32) ratio ranged from 3 to 6.3. SO_2(m/e=64) also contributes to the 32 m/e. The deviation in the calculated ratio is due to the contribution of SO_2 to m/e of O_2 and this contribution cannot quantified accurately. The pulse calbration is also done to ensure that the ratio of N_2 to O_2 is close 3.26.
- The estimated concentration of simulated flue gas mixture from the mass spectrometer will be verified by gas chromatography.

4.7. Nature of adsorbed CO_2 and HCl probing

Figure 35 (a) shows the IR absorbance spectra of adsorbed CO_2 on TEPA/SiO_2 (50/50) sorbent in the presence and in the absence of gas phase CO_2, and after probing the adsorbed CO_2 with vapor phase HCl . The absorbance spectra $A_{CO2\ tot.}$ represent the total adsorbed CO_2 in presence of gas phase CO_2 and $A_{CO2\ str}$ represent the strongly adsorbed CO_2 in the absence of CO_2 (i.e., under flowing Ar). The absorbance spectra of adsrobed CO_2 probed with HCl vapor was represented as $A_{CO2\ Str/HCl}$. The difference between total adsorbed and strongly adsorbed CO_2 gives the information on weakly adsorbed CO_2. The nature of adsorbed CO_2 on amines can be understood by treating total adsorbed CO_2 or strongly adsorbed CO_2 with HCl vapor. The difference spectra in Figure 35 (b) was obtained by plotting $A_{CO2\ tot} - A_{CO2\ str}$ for weakly adsorbed CO_2, and $A_{CO2\ str} - A_{CO2\ str/HCl}$ gives the information on nature of adsorbed CO_2. The spectral range can be divided in to three regions 4000-2800 cm^{-1} A-branch; 2800-1800 cm^{-1}B-branch; and 1800-600 cm^{-1} C-branch. A and B branches represent the ammonium ions and C-branch represents adsorbed CO_2. The detailed band assignments are presented in figure 36.

Figure 36 shows the IR absorbance spectra of total adsorbed CO_2 and strongly adsorbed CO_2 on TEPA/SiO_2 (50/50), PEI/SiO_2 (50/50), and PEI/PEG/SiO_2 (29/19/52) sorbents. The spectra of all the sorbents exhibited identical positions of the bands for the adsorbed CO_2 irrespective of type of amine used and presence of additive PEG-200. The bands produced on different sorbents are identified as carbamates and ammonium ions (NH_3^+/NH_2^+) vide infra. The absorbance spectra on TEPA/SiO_2 (50/50) show an additional band at 1680 cm^{-1} that represents carbamic acid. This indicates that CO_2 adsorption on amines is similar on all sorbents irrespective of the amine used. However, there are differences in the intensities of the bands produced for total adsorbed and strongly adsorbed CO_2 on each sorbent. The IR intensities of the bands produced

due to adsorbed CO_2 and ammonium ions are stronger on TEPA/SiO_2(50/50) compared to PEI/SiO_2 (50/50) with identical amine loadings. The IR intensities of adsorbed CO_2 are stronger than ammonium ions for PEI sorbents, and were increased in presence of PEG-200. The stronger intensity of adsorbed CO_2 bands in PEI/PEG/SiO_2 can be attributed to the positive effect of OH groups in PEG-200. Similar results are observed in liquid thin films. The intensity of the bands produced on TEPA are much stronger than those observed on PEI and PEI/PEG (73/27) thin films. . The rate of increase in intensity of adsorbed CO_2 on powder sorbents follows the order TEPA/SiO_2> PEI/PEG/SiO_2>PEI/SiO_2) and on liquid samples follows the order TEPA>> PEI/PEG ~ PEI. Weakly adsorbed CO_2 on the sorbents was removed by flowing Ar as an inert gas. The depletion of the intensities of adsorbed species in TEPA/SiO_2 (50/50) sorbent was minimal suggesting that this sorbent has strong CO_2-amine interactions. For PEI sorbents the depletion of the intensities of the bands are higher representing weak CO_2-amine interactions. With this observation we suggest that there are differences in the nature of adsorbed CO_2 on amines between TEPA and PEI when dispersed on a solid support. IR absorbance spectra of powder sorbents during batch calibration and TPD shows that increments in concentration of CO_2 in the reaction chamber change the adsorption mode of CO_2 on amines. The results show that increases in CO_2 concentration transforms carbamates into carbamic acid. Carbamic acid requires only one amine site for adsorption of one CO_2 molecule, unlike carbamates which use two amine sites for adsorption. This information is helpful for increasing the efficiency of the existing amine sorbents.

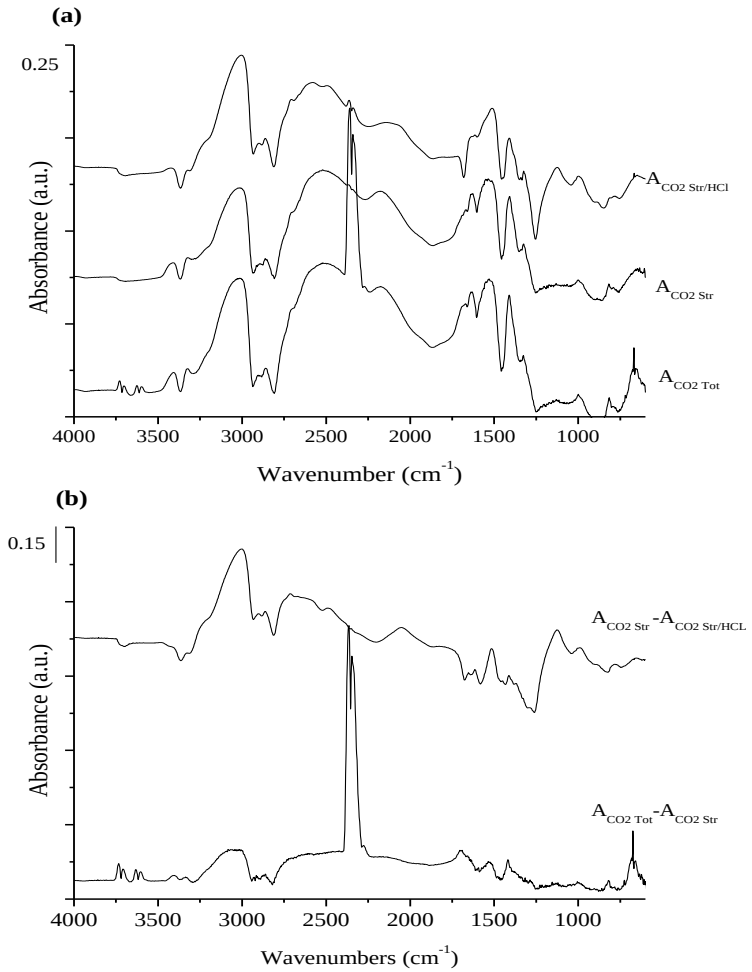

Figure 35: (a) IR absorbance spectra for total adsorbed, strongly adsorbed CO_2 and HCl probing on strongly adsorbed CO_2 for TEPA/SiO_2 (50/50) sorbent. Absorbance spectra were obtained by Abs= -log(I/I_o), where I is the single beam spectra of interest and I_o is the single beam spectra of pretreated sorbent. (b) Weakly adsorbed CO_2 and

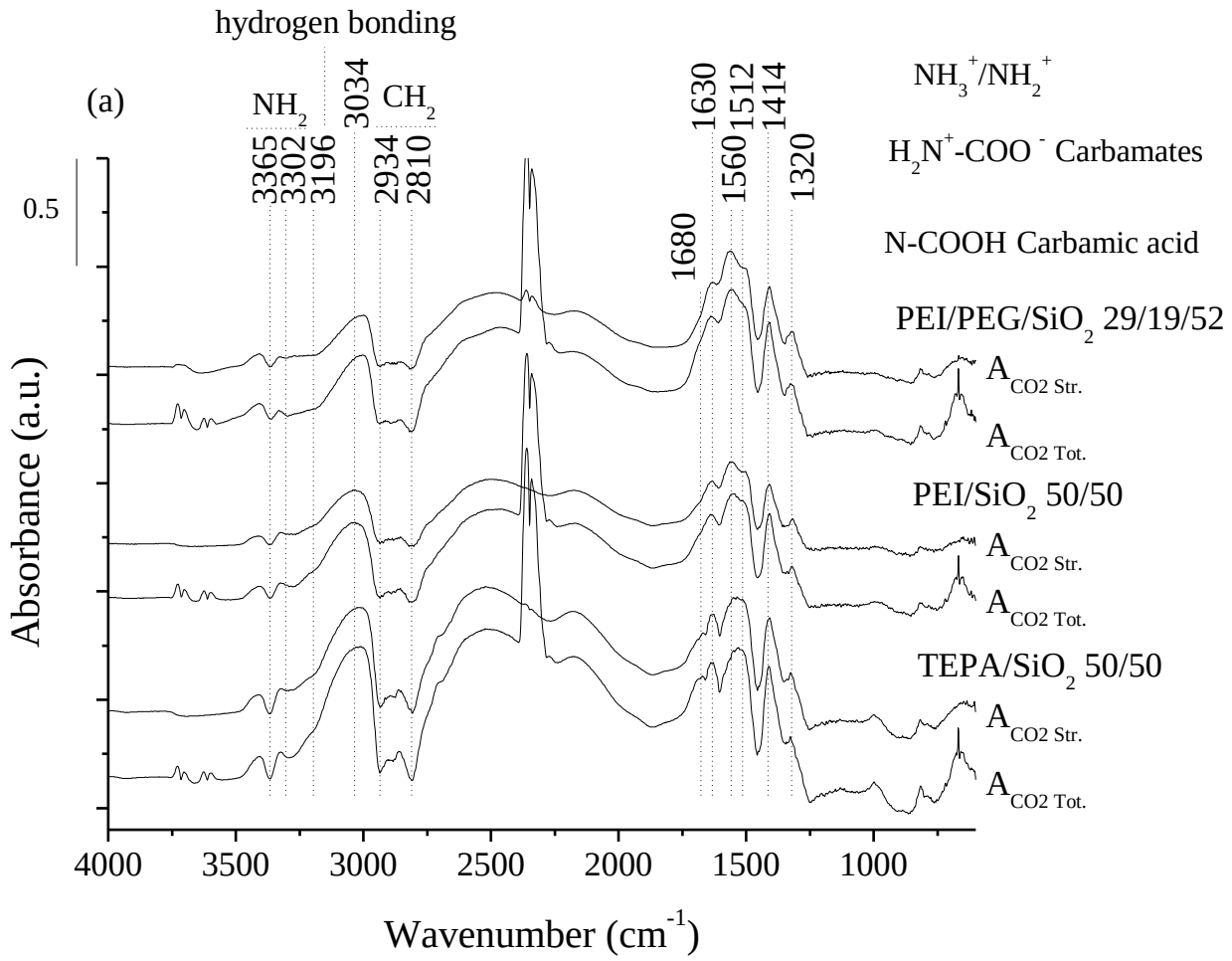

Figure 36: IR absorbance spectra of (a) Total adsorbed and strongly adsorbed CO_2 (b) weakly adsorbed CO_2 on solid sorbents. Absorbance spectra was obtained by Abs= -log(I/Io), where I is the single beam spectra of interest and Io is the single beam spectra of pret

Table 7 summarizes the amount of strongly adsorbed CO_2, CO_2/N ratios, and T_{max} of desorption for liquid thin films and solid sorbents. TEPA present in liquid form and on solid support exhibited more strongly adsorbed CO_2 than PEI counterparts. TEPA/SiO_2 (50/50) sorbent strongly adsorbs 3.56 mmolCO_2 per gram of sorbent, with CO_2/N ratio of 0.27. PEI/SiO_2 (50/50) and PEI/PEG/SiO_2 (29/19/52) exhibit CO_2 capture capacities of 2.07 and 2.08 mmol-str.CO_2/g-sorb. with CO_2/N ratios of 0.18 and 0.31 respectively. Similar strongly adsorbed CO_2 with low PEI loading was achieved by the addition of PEG-200 to the sorbent suggesting the positive effect of OH groups. TPD of liquid amines and solid sorbents showed differences in binding strengths of CO_2 to amine. Liquid TEPA, shows its maximum amount of CO_2 desorption between 90-100 ^oC, and PEI or PEI/PEG show the T_{max} of desorption between 70-80 ^oC. On solid sorbents, this observation was opposite, where TEPA/SiO_2 shows maximum amount of CO_2 desorbed between 80-90 ^oC and PEI sorbents at 100 ^oC. This difference in

binding strength of CO_2 to amines needs to be carefully examined for the preparation of better sorbents for CO_2 capture.

Table 7: CO_2 adsorption characteristic of amine thin films and solid sorbents

	Capture capacity (mmol-str.CO_2 /g-sorb.)	Amine efficiency (CO_2/N)	T_{max} of desorp. (^oC)
Thin film	Desorption at100 ^oC		
TEPA	13.5	0.51	100
PEI	4.94	0.15	80
PEI/PEG (73:27)	9.11	0.39	80
Powder sorbent	Desorption at 130 ^oC		
TEPA/SiO_2 (50/50)	3.56	0.27	90
PEI/SiO_2 (50/50)	2.07	0.18	100
PEI/PEG/SiO_2 (29/19/52)	2.08	0.31	100

HCl was used to probe total and strongly adsorbed CO_2 on the powder sorbents and liquid thin films. The liquids and sorbents exhibit different behaviors when probed with HCl vapor. Figure 37 shows the difference spectra during HCl vapor probing on total and strongly adsorbed CO_2 on (a) TEPA, PEI/PEG thin films, and on (b) TEPA/SiO_2 (50/50) and PEI/PEG/SiO_2 (29/19/52) sorbents. HCl probing on total adsorbed was carried out by flowing CO_2 and the probing on strongly adsorbed was carried out by flowing Ar. The difference spectra for total adsorbed CO_2 and after HCl probing was represented as $A_{CO2\ Tot}$-$A_{CO2\ Tot/HCl}$. The difference spectra for strongly adsobed CO_2 and after HCl probing represented as $A_{CO2\ Str}$-$A_{CO2\ Str/HCl}$. HCl probing on TEPA thin film for total adsorbed CO_2 showed dissapearance of carbamates with formation of bands at 1720 cm^{-1} C=O of carbamic acid, at 3470 cm^{-1} for OH stretching in COOH of carbamic acid, and a broad band at 3100 cm^{-1} for NH_3^+ stretching. The formation of carbamic acid can be explained by the abstraction of the proton from HCl by the carbamate ion as shown in equation 1. HCl probing on TEPA with strongly adsorbed CO_2 showed formation of strong and sharp bands for NH_3^+ ion. The changes suggest that the adsorbed CO_2 was displaced by the strength of HCl as shown in equation 2. The PEI/PEG thin film showed the formation of ammonium ions on total adsorbed and strongly adsorbed CO_2 with only a marginal change. The results elucidate the difference in the nature of adsorbed CO_2 between TEPA and PEI.

The reaction of HCl vapor with adsorbed CO_2 on amines can be represented by the following equations:

Total adsorbed CO_2:

$RNHCOO^- + NH_3^+ + HCl \rightarrow RNHCOOH + NH_3^+ Cl^-$ ……(1)

and strongly adsorbed:

$RNHCOO^- + NH_3^+ + HCl \rightarrow RNH_2 + CO_2 + NH_3^+ Cl^-$ ……(2)

For powder sorbents, the total adsorbed and strongly adsorbed CO_2 produced carbamic acid , OH groups and ammonium ions after the HCl vapor probing. The formation of ammonium ions was strogner for strongly adsorbedbecause in flowing Ar there is no competition between protons and CO_2 to adsorb on amines. The results also show that the formation of ammonium ions are different for TEPA/SiO_2 and PEI/PEG/SiO_2. TEPA/SiO_2 formed a very strong and broad band at 3000 cm^{-1} corresponidng to ammonum ions, while, PEI/PEG/SiO_2 formed a sharper and weaker band. The strong formation of ammonium ions in powder sorbents can be attributed to the availability of free amines on the surface, confirmed by the CO_2/N ratios which are less than the theorotical maximum of 0.5. The free amines can abstract the proton from HCl to form ammonium ions and are be stabilized by the chloride ion. The stronger formation of ammonium ions in TEPA/SiO_2 than in PEI/PEG/SiO_2 can be attributed to the higher amine loading in TEPA/SiO_2 (50/50) compared to PEI/PEG/SiO_2 (29/19/52).

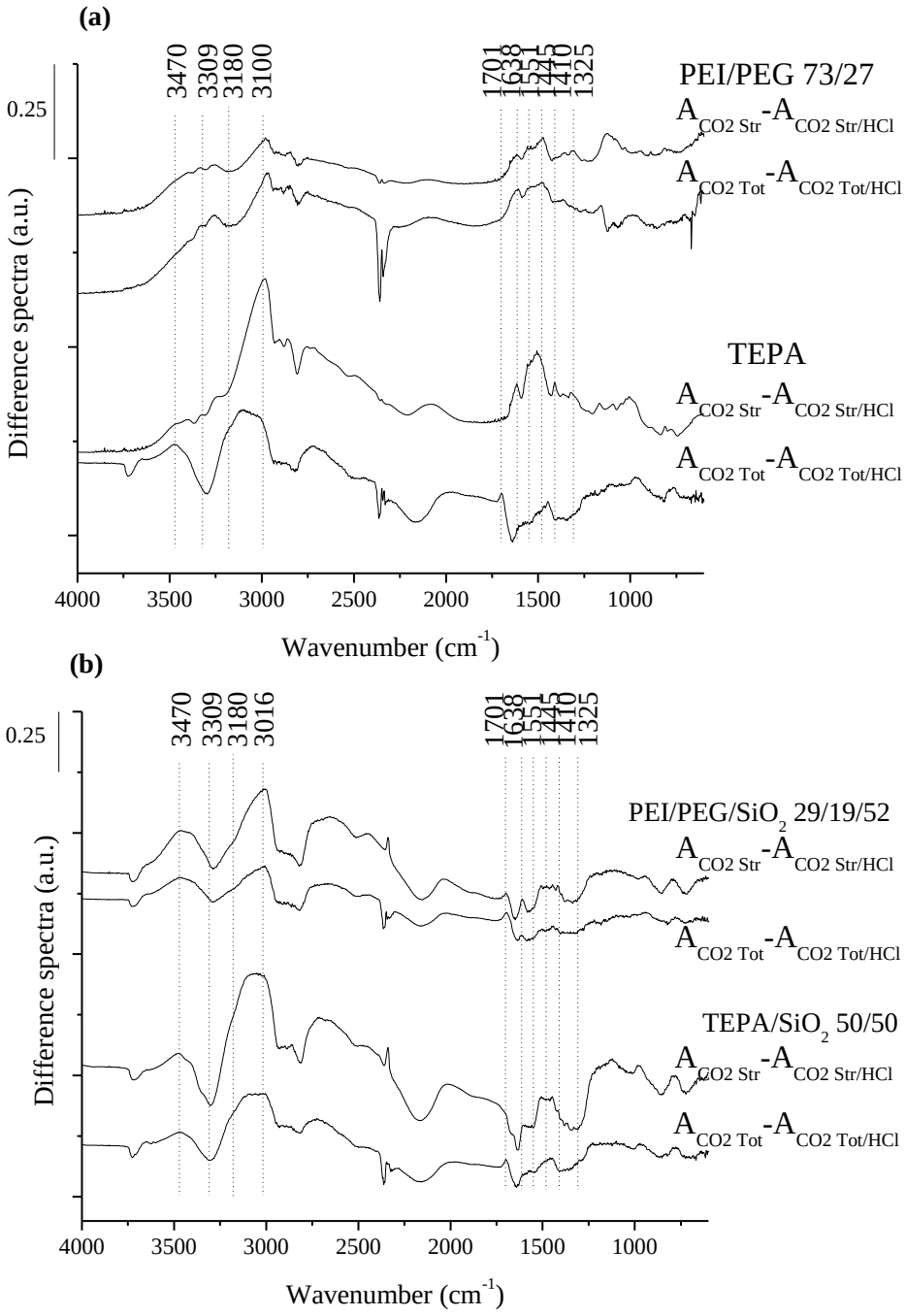

Figure 37: Difference spectra on (a) TEPA and PEI/PEG, (b) TEPA/SiO_2 (50/50) and PEI/PEG/SiO_2 on total adsorbed and strongly adsorbed CO_2 after HCl-vapor treatment

Conclusions:

This work has provided an new tool in determining the capture capacity of amine sorbents by using an insitu FTIR batch calibration. Sorbents with high amounts of strongly adsorbed CO_2, and fast adsorption desorption kinetics were achieved by using low cost TEPA and amorphous

SiO_2. The results showed that the addition of PEG to PEI enhances the CO_2 adsorption capacity at lower temperatures. The results also indicate that adsorbed CO_2 on amines can be changed from carbamate to carbamic acid by increasing the CO_2 concentration, resulting in higher amine efficiencies. HCl probing showed that strongly adsorbed CO_2 transforms to carbamic acid and weakly adsorbed CO_2 will be removed from the amines. The result also showed the difference in nature of adsorbed CO_2 on solids and liquids. HCl probing is a useful method to identify the nature of CO_2-amine interactions, the development of this method requires further investigation for its application in preparing more effective sorbents for CO_2 capture.

5. Conclusions

In-situ FTIR results for liquid films showed that the presence of PEG improved the SO_2 capture capacities and stability of TEPA film. PEG decreases the SO_2-amine interaction, resulting in the decrease in the maximum desorption temperature (T_{max}) of during desorption of SO_2 from TEPA films. The high stability of the TEPA/PEG (1:2) film is attributed to the decrease in the strength of SO_2-amine interaction with increasing amounts of PEG in the film. SO_2 adsorption on TEPA and TEPA/H_2O thin film showed that the addition of water to TEPA minimized the packing between amine through hydrogen bonding between TEPA and water. In the presence of water the adsorption capacity of the TEPA thin films was enhanced, and also the temperature required for desorption of adsorbed species decreased. The results from the fundamental study of SO_2 capture on liquid films are used to design SO_2–resistant amine sorbent. The amine sorbent degraded rapidly with 65% decrease in the initial capture capacity, where as PEG-coated amine sorbent exhibited less degradation. The stability of the sorbent increased with the increase in the concentration of PEG in the coating.

References

(1) Halmann, M.M., Steinberg,M. *Greenhouse Gas Carbon Dioxide Mitigation: Science and Technology*. (Lewis Publishers, Boca Raton), **1998**, 352.

(2) Ertl, G., Knoezinger H. Editors, *Handbook of Heterogeneous Catalysis, 5 Volume Set*. (Wiley-VCH, Weinheim, Germany), **1997**, 2800.

(3) Kang, X., Chuang, S. S. C. *Surfactant Science Series*, **2003**, 108, 25.

(4) Steam - Its generation and uses. *Babcox Wilcox* 41 Ed, **2005**.

(5) Goeppert, A.; Czaun, M.; Surya Prakash, G. K.; Olah, G. A. *Energy & Environmental Science* **2012**, *5*, 7833.

(6) Chang, A. C. C.; Chuang, S. S. C.; Gray, M.; Soong, Y. *Energy & Fuels* **2003**, *17*, 468.

(7) Knofel, C.; Martin, C.; Hornebecq, V.; Llewellyn, P. L. *Journal of Physical Chemistry C* **2009**, *113*, 21726.

(8) Li, P.; Ge, B.; Zhang, S.; Chen, S.; Zhang, Q.; Zhao, Y. *Langmuir* **2008**, *24*, 6567.

(9) Li, P.; Zhang, S.; Chen, S.; Zhang, Q.; Pan, J.; Ge, B. *Journal of Applied Polymer Science* **2008**, *108*, 3851.

(10) Zhang, J.; Han, F.; Wei, X.; Shui, L.; Gong, H.; Zhang, P. *Industrial & Engineering Chemistry Research* **2010**, *49*, 2025.

(11) Wang, X.; Schwartz, V.; Clark, J. C.; Ma, X.; Overbury, S. H.; Xu, X.; Song, C. *Journal of Physical Chemistry C* **2009**, *113*, 7260.

(12) Huang, H. Y.; Yang, R. T.; Chinn, D.; Munson, C. L. *Industrial & Engineering Chemistry Research* **2003**, *42*, 2427.

(13) Fisher, J. C., II; Tanthana, J.; Chuang, S. S. C. *Environ. Prog. Sustainable Energy* **2009**, *28*, 589.

(14) Rocher, N.; Frech, R. *Journal of Physical Chemistry A* **2007**, *111*, 2662.

(15) Pohle, W.; Gauger, D. R. *Journal of Molecular Structure* **2009**, *924-926*, 144.

(16) Khatri, R. A.; Chuang, S. S. C.; Soong, Y.; Gray, M. *Industrial & Engineering Chemistry Research* **2005**, *44*, 3702.

(17) Jackson, P.; Robinson, K.; Puxty, G.; Attalla, M. *Energy Procedia* **2009**, *1*, 985.

(18) Hiyoshi, N.; Yogo, K.; Yashima, T. *Microporous and Mesoporous Materials* **2005**, *84*, 357.

(19) Khatri, R. A.; Chuang, S. S. C.; Soong, Y.; Gray, M. *Energy & Fuels* **2006**, *20*, 1514.

(20) Marcu, I.-C.; Sandulescu, I. *J. Serb. Chem. Soc.* **2004**, *69*, 563.

(21) Shor, A. M.; Rubaylo, A. I. *J. Mol. Struct.* **1997**, *410-411*, 133.

(22) Jiang, B. Q.; Wu, Z. B.; Liu, Y.; Lee, S. C.; Ho, W. K. *J. Phys. Chem. C* **2010**, *114*, 4961.

(23) Zhang, J.; Zhang, P.; Han, F.; Chen, G.; Zhang, L.; Wei, X. *Industrial & Engineering Chemistry Research* **2009**, *48*, 1287.